Chapter 2

Thermodynamics of Separation Operations

Thermodynamic properties and equations play a major role in separation operations, particularly with respect to energy requirements, phase equilibria, and sizing equipment. This chapter discusses applied thermodynamics for separation processes. Equations for energy balances, entropy and availability balances, and for determining phase densities and phase compositions at equilibrium are developed. These involve thermodynamic properties, including specific volume or density, enthalpy, entropy, availability, and fugacities and activities together with their coefficients, all as functions of temperature, pressure, and phase composition. Methods for estimating properties for ideal and nonideal mixtures are summarized. However, this chapter is not a substitute for any of the excellent textbooks on chemical engineering thermodynamics. Furthermore, emphasis here is on fluid phases, with little consideration of solid phases.

2.0 INSTRUCTIONAL OBJECTIVES

After completing this chapter, you should be able to:

- Make energy, entropy, and availability balances around a separation process using the first and second laws of thermodynamics.
- Calculate lost work and second-law efficiency of a separation process.
- Explain the concept of phase equilibria in terms of Gibbs free energy, chemical potential, fugacity, fugacity coefficients, activity, and activity coefficients.
- Understand the concept and usefulness of the equilibrium ratio (*K*-value) for problems involving liquid and/or vapor phases at equilibrium.
- Derive expressions for *K*-values in terms of fugacity coefficients and activity coefficients.
- Write vapor–liquid *K*-value expressions for Raoult's law (ideal), a modified Raoult's law, and Henry's law.
- Calculate density, enthalpy, and entropy of ideal mixtures.
- Utilize graphical correlations to obtain thermodynamic properties of ideal and near-ideal mixtures.
- Use nomographs to estimate vapor–liquid *K*-values of nonideal hydrocarbon and light–gas mixtures.
- Explain how computer programs use equations of state (e.g., Soave-Redlich-Kwong or Peng-Robinson) to compute thermodynamic properties of vapor and liquid mixtures, including *K*-values.
- Explain how computer programs use liquid-phase activity-coefficient correlations (e.g., Wilson, NRTL, UNIQUAC, or UNIFAC) to compute thermodynamic properties, including *K*-values, for nonideal vapor and liquid mixtures at equilibrium.

2.1 ENERGY, ENTROPY, AND AVAILABILITY BALANCES

Most industrial separation operations utilize large quantities of energy in the form of heat and/or shaft work. A study by Mix et al. [1] reports that two quads (1 quad $= 10^{15}$ Btu) of energy were consumed by distillation separations in petroleum, chemical, and natural-gas processing plants in the United States in 1976. This amount of energy was 2.7% of the total U.S. energy consumption of 74.5 quads and is equivalent to the energy obtained from approximately 1 million bbl of crude oil per day over a one-year period. This amount of oil can be compared to 13 million bbl/day, the average amount of crude oil processed by petroleum refineries in the United States in early 1991. At a crude oil price of approximately $40/bbl, the energy consumption by distillation in the United States is approximately $20 trillion per year. Thus, it is of considerable interest to know the extent of energy consumption in a separation process, and to what degree energy requirements might be reduced. Such energy estimates can be made by applying the first and second laws of thermodynamics.

Consider the continuous, steady-state, flow system for a general separation process in Figure 2.1. One or more feed streams flowing into the system are separated into two or

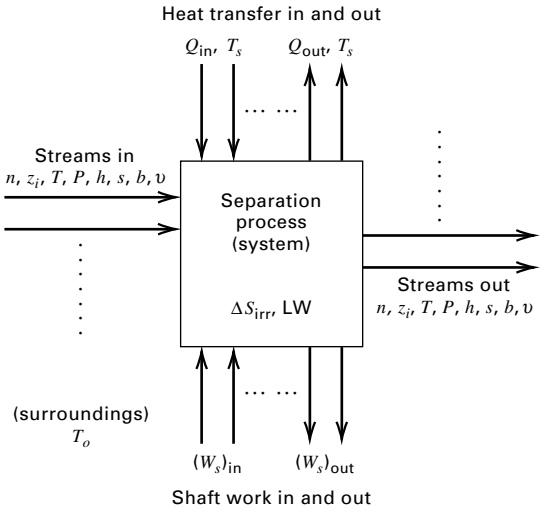

Figure 2.1 General separation system.

more product streams that flow out of the system. For all these streams, we denote the molar flow rates by n, the component mole fractions by z_i, the temperature by T, the pressure by P, the molar enthalpies by h, the molar entropies by s, and the molar availabilities by b. If chemical reactions occur in the process, enthalpies and entropies are referred to the elements, as discussed by Felder and Rousseau [2]; otherwise they can be referred to the compounds. Heat flows in or out of the system are denoted by Q, and shaft work crossing the boundary of the system is denoted by W_s. At steady state, if kinetic, potential, and surface energy changes are neglected, the first law of thermodynamics (also referred to as the conservation of energy or the energy balance), states that the sum of all forms of energy flowing into the system equals the sum of the energy flows leaving the system:

$$\begin{aligned}&(\text{stream enthalpy flows} + \text{heat transfer}\\ &\qquad + \text{shaft work})_{\text{leaving system}} - (\text{stream enthalpy flows}\\ &\qquad + \text{heat transfer} + \text{shaft work})_{\text{entering system}}\\ &= 0\end{aligned}$$

In terms of symbols, the energy balance is given by Eq. (1) in Table 2.1, where all flow rate, heat transfer, and shaft work terms are positive. Molar enthalpies may be positive or negative depending on the reference state.

All separation processes must satisfy the energy balance. Inefficient separation processes require large transfers of heat and/or shaft work both into and out of the process; efficient processes require smaller levels of heat transfer and/or shaft work. The first law of thermodynamics provides no information on energy efficiency, but the second law of thermodynamics (also referred to as the entropy balance), given by Eq. (2) in Table 2.1, does. In words, the steady-state entropy balance is

$$\begin{aligned}&(\text{Stream entropy flows}\\ &\qquad + \text{entropy flows by heat transfer})_{\text{leaving system}}\\ &\qquad - (\text{stream entropy flows}\\ &\qquad + \text{entropy flows by heat transfer})_{\text{entering system}}\\ &= \text{production of entropy by the process}\end{aligned}$$

In the entropy balance equation, the heat sources and sinks in Figure 2.1 are at absolute temperatures T_s. For example, if condensing steam at 150°C supplies heat, Q, to the reboiler of a distillation column, $T_s = 150 + 273 = 423$ K. If cooling water at an average temperature of 30°C removes heat, Q, in a condenser, $T_s = 30 + 273 = 303$ K. Unlike the energy balance, which states that energy is conserved, the entropy balance predicts the production of entropy, ΔS_{irr}, which is the irreversible increase in the entropy of the universe. This term, which must be a positive quantity, is a quantitative measure of the thermodynamic inefficiency of a process. In the limit, as a reversible process is approached, ΔS_{irr} tends to zero. Note that the entropy balance contains no terms related to shaft work.

Although ΔS_{irr} is a measure of energy inefficiency, it is difficult to relate to this measure because it does not have the units of energy/time (power). A more useful measure or process inefficiency can be derived by combining (1) and (2) in Table 2.1 to obtain a combined statement of the first and second laws of thermodynamics, which is given as (3) in Table 2.1. To perform this derivation, it is first necessary to define an infinite source of or sink for heat transfer at the absolute temperature, $T_s = T_0$, of the surroundings. This temperature is typically about 300 K and represents the largest

Table 2.1 Universal Thermodynamic Laws for a Continuous, Steady-State, Flow System

Energy balance:

(1) $$\sum_{\substack{\text{out of}\\ \text{system}}} (nh + Q + W_s) - \sum_{\substack{\text{in to}\\ \text{system}}} (nh + Q + W_s) = 0$$

Entropy balance:

(2) $$\sum_{\substack{\text{out of}\\ \text{system}}} \left(ns + \frac{Q}{T_s}\right) - \sum_{\substack{\text{in to}\\ \text{system}}} \left(ns + \frac{Q}{T_s}\right) = \Delta S_{\text{irr}}$$

Availability balance:

(3) $$\sum_{\substack{\text{in to}\\ \text{system}}} \left[nb + Q\left(1 - \frac{T_0}{T_s}\right) + W_s\right] - \sum_{\substack{\text{out of}\\ \text{system}}} \left[nb + Q\left(1 - \frac{T_0}{T_s}\right) + W_s\right] = \text{LW}$$

Minimum work of separation:

(4) $$W_{\min} = \sum_{\substack{\text{out of}\\ \text{system}}} nb - \sum_{\substack{\text{in to}\\ \text{system}}} nb$$

Second-law efficiency:

(5) $$\eta = \frac{W_{\min}}{\text{LW} + W_{\min}}$$

where $b = h - T_0 s$ = availability function

$\text{LW} = T_0 \Delta S_{\text{irr}}$ = lost work

source of coolant associated with the processing plant being analyzed. This might be the average temperature of cooling water, air, or a nearby river, lake, or ocean. Heat transfer associated with this surrounding coolant and transferred from (or to) the process is termed Q_0. Thus, in both (1) and (2) in Table 2.1, the Q and Q/T_s terms include contributions from Q_0 and Q_0/T_0, respectively.

The derivation of (3) in Table 2.1 can be made, as shown by de Nevers and Seader [3], by combining (1) and (2) to eliminate Q_0. The resulting equation is referred to as an *availability* (or *exergy*) balance, where the term availability means "available for complete conversion to shaft work." The stream availability function, b, as defined by

$$b = h - T_0 s \tag{2-1}$$

is a measure of the maximum amount of stream energy that can be converted into shaft work if the stream is taken to the reference state. It is similar to Gibbs free energy, $g = h - Ts$, but differs in that the infinite surroundings temperature, T_0, appears in the equation instead of the stream temperature, T. Terms in (3) in Table 2.1 containing Q are multiplied by $(1 - T_0/T_s)$, which, as shown in Figure 2.2, is the reversible Carnot heat-engine cycle efficiency, representing the maximum amount of shaft work that can be produced from Q at T_s, where the residual amount of energy $(Q - W_s)$ is transferred as heat to a sink at T_0. Shaft work, W_s, remains at its full value in (3). Thus, although Q and W_s have the same thermodynamic worth in (1) of Table 2.1, heat transfer has less worth in (3). This is because shaft work can be converted completely to heat (by friction), but heat cannot be converted completely to shaft work unless the heat is available at an infinite temperature.

Availability, like entropy, is not conserved in a real, irreversible process. The total availability (i.e., ability to produce shaft work) passing into a system is always greater than the total availability leaving a process. Thus (3) in Table 2.1 is written with the "into system" terms first. The difference

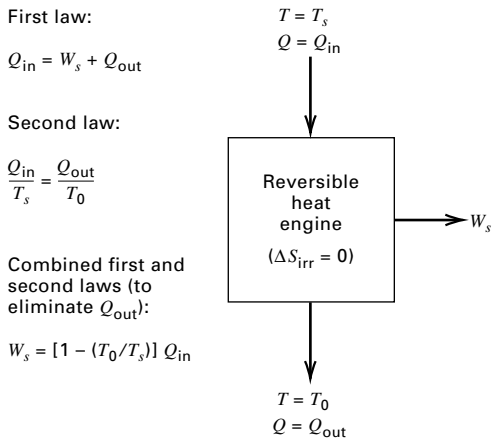

Figure 2.2 Carnot heat engine cycle for converting heat to shaft work.

is the *lost work,* LW, which is also called the loss of availability (or exergy), and is defined by

$$\text{LW} = T_0 \Delta S_{\text{irr}} \tag{2-2}$$

Lost work is always a positive quantity. The greater its value, the greater is the energy inefficiency. In the lower limit, as a reversible process is approached, lost work tends to zero. The lost work has the same units as energy, thus making it easy to attach significance to its numerical value. In words, the steady-state availability balance is

(Stream availability flows + availability of heat + shaft work)$_{\text{entering system}}$ − (stream availability flows + availability of heat + shaft work)$_{\text{leaving system}}$ = loss of availability (lost work)

For any separation process, lost work can be computed from (3) in Table 2.1. Its magnitude depends on the extent of process irreversibilities, which include fluid friction, heat transfer due to finite temperature-driving forces, mass transfer due to finite concentration or activity-driving forces, chemical reactions proceeding at finite displacements from chemical equilibrium, mixing of streams at differing conditions of temperature, pressure, and/or composition, and so on. Thus, to reduce the lost work, driving forces for momentum transfer, heat transfer, mass transfer, and chemical reaction must be reduced. Practical limits to this reduction exist because, as driving forces are decreased, equipment sizes increase, tending to infinitely large sizes as driving forces approach zero.

For a separation process that occurs without chemical reaction, the summation of the stream availability functions leaving the process is usually greater than the same summation for streams entering the process. In the limit for a reversible process (LW = 0), (3) of Table 2.1 reduces to (4), where $W_{\min}$ is the minimum shaft work required to conduct the separation and is equivalent to the difference in the heat transfer and shaft work terms in (3). This minimum work is independent of the nature (or path) of the separation process. The work of separation for an actual irreversible process is always greater than the minimum value computed from (4).

From (3) of Table 2.1, it is seen that as a separation process becomes more irreversible, and thus more energy inefficient, the increasing LW causes the required equivalent work of separation to increase by the same amount. Thus, the equivalent work of separation for an irreversible process is given by the sum of lost work and minimum work of separation. The *second-law efficiency,* therefore, can be defined as

$$\text{(fractional second-law efficiency)} = \left(\frac{\text{minimum work of separation}}{\text{equivalent actual work of separation}} \right)$$

In terms of symbols, the efficiency is given by (5) in Table 2.1.

EXAMPLE 2.1

For the propylene–propane separation of Figure 1.12, using the following thermodynamic properties for certain streams, as estimated from the Soave–Redlich–Kwong equation of state discussed in Section 2.5, and the relations given in Table 2.1, compute in SI units:

(a) The condenser duty, Q_C

(b) The reboiler duty, Q_R

(c) The irreversible entropy production, assuming 303 K for the condenser cooling-water sink and 378 K for the reboiler steam source

(d) The lost work, assuming $T_0 = 303$ K

(e) The minimum work of separation

(f) The second-law efficiency

Stream	Phase Condition	Enthalpy (h), kJ/kmol	Entropy (s), kJ/kmol-K
Feed (F)	Liquid	13,338	−4.1683
Overhead vapor (OV)	Vapor	24,400	24.2609
Distillate (D) and reflux (R)	Liquid	12,243	−13.8068
Bottoms (B)	Liquid	14,687	−2.3886

SOLUTION

Place the condenser (C) cooling water and the reboiler (R) steam outside the distillation system. Thus, Q_C and Q_R cross the boundary of the system. The following calculations are made using the stream flow rates in Figure 1.12 and properties above.

(a) Compute condenser duty from an energy balance around the condenser. From (1), Table 2.1, noting that the overhead-vapor molar flow rate is given by $n_{OV} = n_R + n_D$ and $h_R = h_D$, the condenser duty is

$$\begin{aligned} Q_C &= n_{OV}(h_{OV} - h_R) \\ &= (2{,}293 + 159.2)(24{,}400 - 12{,}243) \\ &= 29{,}811{,}000 \text{ kJ/h} \end{aligned}$$

(b) Compute reboiler duty from an energy balance around the entire distillation operation. (An energy balance around the reboiler cannot be made because data are not given for the boilup rate.) From (1), Table 2.1,

$$\begin{aligned} Q_R &= n_D h_D + n_B h_B + Q_C - n_F h_F \\ &= 159.2(12{,}243) + 113(14{,}687) \\ &\quad + 29{,}811{,}000 - 272.2(13{,}338) \\ &= 29{,}789{,}000 \text{ kJ/h} \end{aligned}$$

(c) Compute the production of entropy from an entropy balance around the entire distillation system. From Eq. (2), Table 2.1,

$$\begin{aligned} \Delta S_{\text{irr}} &= n_D s_D + n_B s_B + Q_C/T_C - n_F s_F - Q_R/T_R \\ &= 159.2(-13.8068) + 113(-2.3886) + 29{,}811{,}000/303 \\ &\quad - 272.2(-4.1683) - 29{,}789{,}000/378 \\ &= 18{,}246 \text{ kJ/h–K} \end{aligned}$$

(d) Compute lost work from its definition at the bottom of Table 2.1:

$$\begin{aligned} \text{LW} &= T_0 \Delta S_{\text{irr}} \\ &= 303(18{,}246) = 5{,}529{,}000 \text{ kJ/h} \end{aligned}$$

Alternatively, compute lost work from an availability balance around the entire distillation system. From (3), Table 2.1, where the availability function, b, is defined near the bottom of Table 2.1,

$$\begin{aligned} \text{LW} &= n_F b_F + Q_R(1 - T_0/T_R) \\ &\quad - n_D b_D - n_B b_B - Q_C(1 - T_0/T_C) \\ &= 272.2[13{,}338 - (303)(-4.1683)] \\ &\quad + 29{,}789{,}000(1 - 303/378) \\ &\quad - 159.2[12{,}243 - (303)(-13.8068)] \\ &\quad - 113[14{,}687 - (303)(-2.3886)] \\ &\quad - 29{,}811{,}000(1 - 303/303) \\ &= 5{,}529{,}000 \text{ kJ/h} \quad \text{(same result)} \end{aligned}$$

(e) Compute the minimum work of separation for the entire distillation system. From (4), Table 2.1,

$$\begin{aligned} W_{\min} &= n_D b_D + n_B b_B - n_F b_F \\ &= 159.2[12{,}243 - (303)(-13.8068)] \\ &\quad + 113[14{,}687 - (303)(-2.3886)] \\ &\quad - 272.2[13{,}338 - (303)(-4.1683)] \\ &= 382{,}100 \text{ kJ/h} \end{aligned}$$

(f) Compute the second-law efficiency for the entire distillation system. From (5), Table 2.1,

$$\begin{aligned} \eta &= \frac{W_{\min}}{LW + W_{\min}} \\ &= \frac{382{,}100}{5{,}529{,}000 + 382{,}100} \\ &= 0.0646 \quad \text{or} \quad 6.46\% \end{aligned}$$

This low second-law efficiency is typical of a difficult distillation separation, which in this case requires 150 theoretical stages with a reflux ratio of almost 15 times the distillate rate.

2.2 PHASE EQUILIBRIA

Analysis of separations equipment frequently involves the assumption of phase equilibria as expressed in terms of Gibbs free energy, chemical potentials, fugacities, or activities. For each phase in a multiphase, multicomponent system, the total Gibbs free energy is

$$G = G(T, P, N_1, N_2, \ldots, N_C)$$

where N_i = moles of species i. At equilibrium, the total G for all phases is a minimum, and methods for determining this minimum are referred to as *free-energy minimization techniques.* Gibbs free energy is also the starting point for the derivation of commonly used equations for expressing phase equilibria. From classical thermodynamics, the total differential of G is given by

$$dG = -S\,dT + V\,dP + \sum_{i=1}^{C} \mu_i\,dN_i \qquad (2\text{-}3)$$

where μ_i is the chemical potential or partial molar Gibbs free energy of species i. When (2-3) is applied to a closed system consisting of two or more phases in equilibrium at uniform temperature and pressure, where each phase is an open system capable of mass transfer with another phase, then

$$dG_{\text{system}} = \sum_{p=1}^{N} \left[\sum_{i=1}^{C} \mu_i^{(p)} dN_i^{(p)} \right]_{P,T} \tag{2-4}$$

where the superscript (p) refers to each of N phases in equilibrium. Conservation of moles of each species, in the absence of chemical reaction, requires that

$$dN_i^{(1)} = -\sum_{p=2}^{N} dN_i^{(p)} \tag{2-5}$$

which, upon substitution into (2-4), gives

$$\sum_{p=2}^{N} \left[\sum_{i=1}^{C} \left(\mu_i^{(p)} - \mu_i^{(1)} \right) dN_i^{(p)} \right] = 0 \tag{2-6}$$

With $dN_i^{(1)}$ eliminated in (2-6), each $dN_i^{(p)}$ term can be varied independently of any other $dN_i^{(p)}$ term. But this requires that each coefficient of $dN_i^{(p)}$ in (2-6) be zero. Therefore,

$$\mu_i^{(1)} = \mu_i^{(2)} = \mu_i^{(3)} = \cdots = \mu_i^{(N)} \tag{2-7}$$

Thus, the chemical potential of a particular species in a multicomponent system is identical in all phases at physical equilibrium.

Fugacities and Activity Coefficients

Chemical potential cannot be expressed as an absolute quantity, and the numerical values of chemical potential are difficult to relate to more easily understood physical quantities. Furthermore, the chemical potential approaches an infinite negative value as pressure approaches zero. For these reasons, the chemical potential is not favored for phase equilibria calculations. Instead, fugacity, invented by G. N. Lewis in 1901, is employed as a surrogate.

The partial fugacity of species i in a mixture is like a pseudo-pressure, defined in terms of the chemical potential by

$$\bar{f}_i = C \exp\left(\frac{\mu_i}{RT} \right) \tag{2-8}$$

where C is a temperature-dependent constant. Regardless of the value of C, it is shown by Prausnitz, Lichtenthaler, and Azevedo [4] that (2-7) can be replaced with

$$\bar{f}_i^{(1)} = \bar{f}_i^{(2)} = \bar{f}_i^{(3)} = \cdots = \bar{f}_i^{(N)} \tag{2-9}$$

Thus, at equilibrium, a given species has the same partial fugacity in each existing phase. This equality, together with equality of phase temperatures and pressures,

$$T^{(1)} = T^{(2)} = T^{(3)} = \cdots = T^{(N)} \tag{2-10}$$

and

$$P^{(1)} = P^{(2)} = P^{(3)} = \cdots = P^{(N)} \tag{2-11}$$

constitutes the required conditions for phase equilibria. For a pure component, the partial fugacity, $\bar{f}_i$, becomes the pure-component fugacity, f_i. For a pure, ideal gas, fugacity is equal to the pressure, and for a component in an ideal-gas mixture, the partial fugacity is equal to its partial pressure, $p_i = y_i P$. Because of the close relationship between fugacity and pressure, it is convenient to define their ratio for a pure substance as

$$\phi_i = \frac{f_i}{P} \tag{2-12}$$

where ϕ_i is the pure-species fugacity coefficient, which has a value of 1.0 for an ideal gas. For a mixture, partial fugacity coefficients are defined by

$$\bar{\phi}_{iV} \equiv \frac{\bar{f}_{iV}}{y_i P} \tag{2-13}$$

$$\bar{\phi}_{iL} \equiv \frac{\bar{f}_{iL}}{x_i P} \tag{2-14}$$

such that as ideal-gas behavior is approached, $\bar{\phi}_{iV} \to 1.0$ and $\bar{\phi}_{iL} \to P_i^s / P$, where P_i^s = vapor (saturation) pressure.

At a given temperature, the ratio of the partial fugacity of a component to its fugacity in some defined standard state is termed the *activity.* If the standard state is selected as the pure species at the same pressure and phase condition as the mixture, then

$$a_i \equiv \frac{\bar{f}_i}{f_i^o} \tag{2-15}$$

Since at phase equilibrium, the value of f_i^o is the same for each phase, substitution of (2-15) into (2-9) gives another alternative condition for phase equilibria,

$$a_i^{(1)} = a_i^{(2)} = a_i^{(3)} = \cdots = a_i^{(N)} \tag{2-16}$$

For an ideal solution, $a_{iV} = y_i$ and $a_{iL} = x_i$.

To represent departure of activities from mole fractions when solutions are nonideal, *activity coefficients* based on concentrations in mole fractions are defined by

$$\gamma_{iV} \equiv \frac{a_{iV}}{y_i} \tag{2-17}$$

$$\gamma_{iL} \equiv \frac{a_{iL}}{x_i} \tag{2-18}$$

For ideal solutions, $\gamma_{iV} = 1.0$ and $\gamma_{iL} = 1.0$.

For convenient reference, thermodynamic quantities that are useful in phase equilibria calculations are summarized in Table 2.2.

Table 2.2 Thermodynamic Quantities for Phase Equilibria

Thermodynamic Quantity	Definition	Physical Significance	Limiting Value for Ideal Gas and Ideal Solution
Chemical potential	$\mu_i \equiv \left(\frac{\partial G}{\partial N_i}\right)_{P,T,N_j}$	Partial molar free energy, $\bar{g}_i$	$\mu_i = \bar{g}_i$
Partial fugacity	$\bar{f}_i \equiv C \exp\left(\frac{\mu_i}{RT}\right)$	Thermodynamic pressure	$\bar{f}_{iV} = y_i P$ $\bar{f}_{iL} = x_i P_i^s$
Fugacity coefficient of a pure species	$\phi_i \equiv \frac{f_i}{P}$	Deviation to fugacity due to pressure	$\phi_{iV} = 1.0$ $\phi_{iL} = \frac{P_i^s}{P}$
Partial fugacity coefficient of a species in a mixture	$\bar{\phi}_{iV} \equiv \frac{\bar{f}_{iV}}{y_i P}$ $\bar{\phi}_{iL} \equiv \frac{\bar{f}_{iL}}{x_i P}$	Deviations to fugacity due to pressure and composition	$\bar{\phi}_{iV} = 1.0$ $\bar{\phi}_{iL} = \frac{P_i^s}{P}$
Activity	$a_i \equiv \frac{\bar{f}_i}{f_i^o}$	Relative thermodynamic pressure	$a_{iV} = y_i$ $a_{iL} = x_i$
Activity coefficient	$\gamma_{iV} \equiv \frac{a_{iV}}{y_i}$ $\gamma_{iL} \equiv \frac{a_{iL}}{x_i}$	Deviation to fugacity due to composition	$\gamma_{iV} = 1.0$ $\gamma_{iL} = 1.0$

K-Values

A *phase-equilibrium ratio* is the ratio of mole fractions of a species present in two phases at equilibrium. For the vapor–liquid case, the constant is referred to as the *K-value* (vapor–liquid equilibrium ratio or *K*-factor):

$$K_i \equiv \frac{y_i}{x_i} \tag{2-19}$$

For the liquid–liquid case, the ratio is referred to as the distribution coefficient or liquid–liquid equilibrium ratio:

$$K_{D_i} \equiv \frac{x_i^{(1)}}{x_i^{(2)}} \tag{2-20}$$

For equilibrium-stage calculations involving the separation of two or more components, separation factors, like (1-4), are defined by forming ratios of equilibrium ratios. For the vapor–liquid case, *relative volatility* is defined by

$$\alpha_{ij} \equiv \frac{K_i}{K_j} \tag{2-21}$$

For the liquid–liquid case, the *relative selectivity* is

$$\beta_{ij} \equiv \frac{K_{D_i}}{K_{D_j}} \tag{2-22}$$

Equilibrium ratios can be expressed by the quantities in Table 2.2 in a variety of rigorous formulations. However, the only ones of practical interest are developed as follows. For vapor–liquid equilibrium, (2-9) becomes, for each component,

$$\bar{f}_{iV} = \bar{f}_{iL}$$

To form an equilibrium ratio, these partial fugacities are commonly replaced by expressions involving mole fractions as derived from the definitions in Table 2.2:

$$\bar{f}_{iL} = \gamma_{iL} x_i f_{iL}^o \tag{2-23}$$

or

$$\bar{f}_{iL} = \bar{\phi}_{iL} x_i P \tag{2-24}$$

and

$$\bar{f}_{iV} = \bar{\phi}_{iV} y_i P \tag{2-25}$$

If (2-24) and (2-25) are used with (2-19), a so-called *equation-of-state form* of the *K*-value is obtained:

$$K_i = \frac{\bar{\phi}_{iL}}{\bar{\phi}_{iV}} \tag{2-26}$$

This expression has received considerable attention, with applications of importance being the Starling modification of the Benedict, Webb, and Rubin (B–W–R–S) equation of state [5], the Soave modification of the Redlich–Kwong (S–R–K or R–K–S) equation of state [6], the Peng–Robinson (P–R) equation of state [7], and the Plöcker et al. modification of the Lee–Kesler (L–K–P) equation of state [8].

If (2-23) and (2-25) are used, a so-called *activity coefficient form* of the *K*-value is obtained:

$$K_i = \frac{\gamma_{iL} f_{iL}^o}{\bar{\phi}_{iV} P} = \frac{\gamma_{iL} \phi_{iL}}{\bar{\phi}_{iV}} \tag{2-27}$$

Table 2.3 Useful Expressions for Estimating K-Values for Vapor–Liquid Equilibria ($K_i \equiv y_i/x_i$)

	Equation	Recommended Application
Rigorous forms:		
(1) Equation-of-state	$K_i = \dfrac{\bar{\phi}_{iL}}{\bar{\phi}_{iV}}$	Hydrocarbon and light gas mixtures from cryogenic temperatures to the critical region
(2) Activity coefficient	$K_i = \dfrac{\gamma_{iL}\phi_{iL}}{\bar{\phi}_{iV}}$	All mixtures from ambient to near-critical temperature
Approximate forms:		
(3) Raoult's law (ideal)	$K_i = \dfrac{P_i^s}{P}$	Ideal solutions at near-ambient pressure
(4) Modified Raoult's law	$K_i = \dfrac{\gamma_{iL}P_i^s}{P}$	Nonideal liquid solutions at near-ambient pressure
(5) Poynting correction	$K_i = \gamma_{iL}\phi_{iV}^s\left(\dfrac{P_i^s}{P}\right)\exp\left(\dfrac{1}{RT}\displaystyle\int_{P_i^s}^{P} v_{iL}\,dP\right)$	Nonideal liquid solutions at moderate pressure and below the critical temperature
(6) Henry's law	$K_i = \dfrac{H_i}{P}$	Low-to-moderate pressures for species at supercritical temperature

Since 1960, (2-27) has received considerable attention with applications to important industrial systems presented by Chao and Seader (C–S) [9], with a modification by Grayson and Streed [10].

Table 2.3 is a summary of useful formulations for estimating K-values for vapor–liquid equilibrium. Included are the two rigorous expressions given by (2-26) and (2-27), from which the other approximate formulations are derived. The so-called Raoult's law or ideal K-value is obtained from (2-27) by substituting from Table 2.2, for an ideal gas and ideal gas and liquid solutions, $\gamma_{iL} = 1.0$, $\phi_{iL} = P_i^s/P$, and $\bar{\phi}_{iV} = 1.0$. The modified Raoult's law relaxes the assumption of an ideal liquid solution by including the liquid-phase activity coefficient. The Poynting-correction form for moderate pressures is obtained by approximating the pure-component liquid fugacity coefficient in (2-27) by the expression

$$\phi_{iL} = \phi_{iV}^s \frac{P_i^s}{P} \exp\left(\frac{1}{RT}\int_{P_i^s}^{P} v_{iL}\,dP\right) \tag{2-28}$$

where the exponential term is the Poynting factor or correction. If the liquid molar volume is reasonably constant over the pressure range, the integral in (2-28) becomes $v_{iL}(P - P_i^s)$. For a light gas species, whose critical temperature is less than the system temperature, the Henry's law form for the K-value is convenient provided that a value of H_i, the empirical Henry's law coefficient, is available. This constant for a particular species, i, depends on liquid-phase composition, temperature, and pressure. As pointed out in other chapters, other forms of Henry's law are used besides the one in Table 2.3. Included in Table 2.3 are recommendations for the application of each of the vapor–liquid K-value expressions.

Regardless of which thermodynamic formulation is used for estimating K-values, the accuracy depends on the particular correlations used for the thermodynamic properties required (i.e., vapor pressure, activity coefficient, and fugacity coefficients). For practical applications, the choice of K-value formulation is a compromise among considerations of accuracy, complexity, convenience, and past experience.

For liquid–liquid equilibria, (2-9) becomes

$$\bar{f}_{iL}^{(1)} = \bar{f}_{iL}^{(2)} \tag{2-29}$$

where superscripts (1) and (2) refer to the two immiscible liquid phases. A rigorous formulation for the distribution coefficient is obtained by combining (2-23) with (2-20) to obtain an expression involving only activity coefficients:

$$K_{D_i} = \frac{x_i^{(1)}}{x_i^{(2)}} = \frac{\gamma_{iL}^{(2)} f_{iL}^{o(2)}}{\gamma_{iL}^{(1)} f_{iL}^{o(1)}} = \frac{\gamma_{iL}^{(2)}}{\gamma_{iL}^{(1)}} \tag{2-30}$$

For vapor–solid equilibria, a useful formulation can be derived if the solid phase consists of just one of the components of the vapor phase. In that case, the combination of (2-9) and (2-25) gives

$$f_{iS} = \bar{\phi}_{iV} y_i P \tag{2-31}$$

At low pressure, $\bar{\phi}_{iV} = 1.0$ and the solid fugacity can be approximated by the vapor pressure of the solid to give for the vapor-phase mole fraction of the component forming the solid phase:

$$y_i = \frac{(P_i^s)_{\text{solid}}}{P} \tag{2-32}$$

For liquid–solid equilibria, a similar useful formulation can be derived if again the solid phase is a pure component. Then the combination of (2-9) and (2-23) gives

$$f_{iS} = \gamma_{iL} x_i f_{iL}^o \tag{2-33}$$

At low pressure, the solid fugacity can be approximated by vapor pressure to give, for the component in the solid phase,

$$x_i = \frac{(P_i^s)_{\text{solid}}}{\gamma_{iL}(P_i^s)_{\text{liquid}}} \tag{2-34}$$

EXAMPLE 2.2

Estimate the *K*-values of a vapor-liquid mixture of water and methane at 2 atm total pressure for temperatures of 20 and 80°C.

SOLUTION

At the conditions of temperature and pressure, water will exist mainly in the liquid phase and will follow Raoult's law, as given in Table 2.3. Because methane has a critical temperature of −82.5°C, well below the temperatures of interest, it will exist mainly in the vapor phase and follow Henry's law, in the form given in Table 2.3. From *Perry's Chemical Engineers' Handbook,* 6th ed., pp. 3-237 and 3-103, the following vapor pressure data for water and Henry's law coefficients for CH_4 are obtained:

T, °C	P^s for H_2O, atm	*H* for CH_4, atm
20	0.02307	3.76×10^4
80	0.4673	6.82×10^4

K-values for water and methane are estimated from (3) and (6), respectively, in Table 2.3, using $P = 2$ atm, with the following results:

T, °C	K_{H_2O}	K_{CH_4}
20	0.01154	18,800
80	0.2337	34,100

The above *K*-values confirm the assumptions of the phase distribution of the two species. The *K*-values for H_2O are low, but increase rapidly with increasing temperature. The *K*-values for methane are extremely high and do not change rapidly with temperature for this example.

2.3 IDEAL-GAS, IDEAL-LIQUID-SOLUTION MODEL

Design procedures for separation equipment require numerical values for phase enthalpies, entropies, densities, and phase–equilibrium ratios. Classical thermodynamics provides a means for obtaining these quantities in a consistent manner from *P*–*v*–*T* relationships, which are usually referred to as *equation-of-state models*. The simplest model applies when both liquid and vapor phases are ideal solutions (all activity coefficients equal 1.0) and the vapor is an ideal gas. Then the thermodynamic properties can be computed from unary constants for each of the species in the mixture in a relatively straightforward manner using the equations given in Table 2.4. In general, these ideal equations apply only at near-ambient pressure, up to about 50 psia (345 kPa), for mixtures of isomers or components of similar molecular structure.

For the vapor, the molar volume and mass density are computed from (1), the ideal-gas law in Table 2.4, which involves the molecular weight, *M*, of the mixture and the universal gas constant, *R*. For a mixture, the ideal-gas law assumes that both Dalton's law of additive partial pressures and Amagat's law of additive pure-species volumes apply.

The molar vapor enthalpy is computed from (2) by integrating, for each species, an equation in temperature for the zero-pressure heat capacity at constant pressure, $C_{P_V}^o$, starting from a reference (datum) temperature, T_0, to the temperature of interest, and then summing the resulting species vapor enthalpies on a mole-fraction basis. Typically, T_0 is taken as 0 K or 25°C. Although the reference pressure is zero, pressure has no effect on the enthalpy of an ideal gas. A common empirical representation of the effect of

Table 2.4 Thermodynamic Properties for Ideal Mixtures

Ideal gas and ideal-gas solution:

(1) $$v_V = \frac{V}{\sum_{i=1}^{C} N_i} = \frac{M}{\rho_V} = \frac{RT}{P}, \qquad M = \sum_{i=1}^{C} y_i M_i$$

(2) $$h_V = \sum_{i=1}^{C} y_i \int_{T_0}^{T} \left(C_P^o\right)_{iV} dT = \sum_{i=1}^{C} y_i h_{iv}^o$$

(3) $$s_V = \sum_{i=1}^{C} y_i \int_{T_0}^{T} \frac{(C_P^o)_{iV}}{T} dT - R \ln\left(\frac{P}{P_0}\right) - R \sum_{i=1}^{C} y_i \ln y_i$$

where the first term is s_V^o

Ideal-liquid solution:

(4) $$v_L = \frac{V}{\sum_{i=1}^{C} N_i} = \frac{M}{\rho_L} = \sum_{i=1}^{C} x_i v_{iL}, \qquad M = \sum_{i=1}^{C} x_i M_i$$

(5) $$h_L = \sum_{i=1}^{C} x_i \left(h_{iV}^o - \Delta H_i^{\text{vap}}\right)$$

(6) $$s_L = \sum_{i=1}^{C} x_i \left[\int_{T_0}^{T} \frac{(C_P^o)_{iV}}{T}\, dT - \frac{\Delta H_i^{\text{vap}}}{T}\right] - R \ln\left(\frac{P}{P_0}\right) - R \sum_{i=1}^{C} x_i \ln x_i$$

Vapor–liquid equilibria:

(7) $$K_i = \frac{P_i^s}{P}$$

Reference conditions (datum): *h*, ideal gas at T_0 and zero pressure; *s*, ideal gas at T_0 and 1 atm pressure.

Refer to elements if chemical reactions occur; otherwise refer to components.

temperature on the zero-pressure vapor heat capacity of a pure component is the following fourth-degree polynomial equation:

$$C^o_{P_V} = [a_0 + a_1 T + a_2 T^2 + a_3 T^3 + a_4 T^4]R \quad (2\text{-}35)$$

where the constants a_k depend on the species. Values of the constants for hundreds of compounds, with T in K, are tabulated by Poling, Prausnitz, and O'Connell [11]. Because $C_P = dh/dT$, (2-35) can be integrated for each species to give the ideal-gas species molar enthalpy:

$$h^o_V = \int_{T_0}^{T} C^o_{P_V}\, dT = \sum_{k=1}^{5} \frac{a_{k-1}(T^k - T_0^k)R}{k} \quad (2\text{-}36)$$

The vapor molar entropy is computed from (3) in Table 2.4 by integrating $C^o_{P_V}/T$ from T_0 to T for each species, summing on a mole-fraction basis, adding a term for the effect of pressure referenced to a datum pressure, P_0, which is generally taken to be 1 atm (101.3 kPa), and adding a term for the entropy change of mixing. Unlike the ideal vapor enthalpy, the ideal vapor entropy includes terms for the effects of pressure and mixing. The reference pressure is not taken to be zero, because the entropy is infinity at zero pressure. If (2-35) is used for the heat capacity,

$$\int_{T_0}^{T} \left(\frac{C^o_{P_V}}{T}\right) dT = \left[a_0 \ln\left(\frac{T}{T_0}\right) + \sum_{k=1}^{4} \frac{a_k(T^k - T_0^k)}{k}\right] R \quad (2\text{-}37)$$

The liquid molar volume and mass density are computed from the pure species molar volumes using (4) in Table 2.4 and the assumption of additive volumes (not densities). The effect of temperature on pure-component liquid density from the freezing point to the critical region at saturation pressure is correlated well by the empirical two-constant equation of Rackett [12]:

$$\rho_L = A B^{-(1-T/T_c)^{2/7}} \quad (2\text{-}38)$$

where values of the constants A, B, and the critical temperature, T_c, are tabulated for approximately 700 organic compounds by Yaws et al. [13].

The vapor pressure of a pure liquid species is well represented over a wide range of temperature from below the normal boiling point to the critical region by an empirical extended Antoine equation:

$$\ln P^s = k_1 + k_2/(k_3 + T) + k_4 T + k_5 \ln T + k_6 T^{k_7} \quad (2\text{-}39)$$

where the constants k_k depend on the species. Values of the constants for hundreds of compounds are built into the physical-property libraries of all computer-aided process simulation and design programs. Constants for other empirical vapor-pressure equations are tabulated for hundreds of compounds by Poling et al. [11]. At low pressures, the enthalpy of vaporization is given in terms of vapor pressure by classical thermodynamics:

$$\Delta H^{\text{vap}} = RT^2 \left(\frac{d \ln P^s}{dT}\right) \quad (2\text{-}40)$$

If (2-39) is used for the vapor pressure, (2-40) becomes

$$\Delta H^{\text{vap}} = RT^2 \left[-\frac{k_2}{(k_3 + T)^2} + k_4 + \frac{k_5}{T} + k_7 k_6 T^{k_7 - 1}\right] \quad (2\text{-}41)$$

The enthalpy of an ideal-liquid mixture is obtained by subtracting the molar enthalpy of vaporization from the ideal vapor molar enthalpy for each species, as given by (2-36), and summing these, as shown by (5) in Table 2.4. The entropy of the ideal-liquid mixture, given by (6), is obtained in a similar manner from the ideal-gas entropy by subtracting the molar entropy of vaporization, given by $\Delta H^{\text{vap}}/T$.

The final equation in Table 2.4 gives the expression for the ideal K-value, previously included in Table 2.3. Although it is usually referred to as the Raoult's law K-value, where Raoult's law is given by

$$p_i = x_i P^s_i \quad (2\text{-}42)$$

the assumption of Dalton's law is also required:

$$p_i = y_i P \quad (2\text{-}43)$$

Combination of (2-42) and (2-43) gives the Raoult's law K-value:

$$K_i \equiv \frac{y_i}{x_i} = \frac{P^s_i}{P} \quad (2\text{-}44)$$

The extended Antoine equation, (2-39) (or some other suitable expression), can be used to estimate vapor pressure. Note that the ideal K-value is independent of phase compositions, but is exponentially dependent on temperature, because of the vapor pressure, and inversely proportional to pressure. From (2-21), the relative volatility using (2-44) is independent of pressure.

EXAMPLE 2.3

Styrene is manufactured by catalytic dehydrogenation of ethylbenzene, followed by vacuum distillation to separate styrene from unreacted ethylbenzene [14]. Typical conditions for the feed to an industrial distillation unit are 77.5°C (350.6 K) and 100 torr (13.33 kPa) with the following vapor and liquid flows

at equilibrium:

	n, kmol/h	
Component	**Vapor**	**Liquid**
Ethylbenzene (EB)	76.51	27.31
Styrene (S)	61.12	29.03

Based on the property constants given below, and assuming that the ideal-gas, ideal-liquid-solution model of Table 2.4 is suitable at this low pressure, estimate values of v_V, ρ_V, h_V, s_V, v_L, ρ_L, h_L, and s_L in SI units, and the K-values and relative volatility.

Property Constants for (2-35), (2-38), (2-39)
(In all cases, T is in K)

	Ethylbenzene	Styrene
M, kg/kmol	106.168	104.152
$C^o_{P_V}$, J/kmol-K:		
a_0R	−43,098.9	−28,248.3
a_1R	707.151	615.878
a_2R	−0.481063	−0.40231
a_3R	1.30084×10^{-4}	9.93528×10^{-5}
a_4R	0	0
P^s, Pa:		
k_1	86.5008	130.542
k_2	−7,440.61	−9,141.07
k_3	0	0
k_4	0.00623121	0.0143369
k_5	−9.87052	−17.0918
k_6	4.13065×10^{-18}	1.8375×10^{-18}
k_7	6	6
ρ_L, kg/m^3:		
A	289.8	299.2
B	0.268	0.264
T_c, K	617.9	617.1

$R = 8.314$ kJ/kmol-K or kPa-m^3/kmol-K = 8,314 J/kmol-K

SOLUTION

Phase mole-fraction compositions and average molecular weights: From $y_i = (n_{iV})/n_V$, $x_i = (n_{iL})/n_L$,

	Ethylbenzene	Styrene
y	0.5559	0.4441
x	0.4848	0.5152

From (1), Table 2.4,

$$M_V = (0.5559)(106.168) + (0.4441)(104.152) = 105.27$$
$$M_L = (0.4848)(106.168) + (0.5152)(104.152) = 105.13$$

Vapor molar volume and density: From (1), Table 2.4,

$$v_V = \frac{RT}{P} = \frac{(8.314)(350.65)}{(13.332)} = 219.2 \text{ m}^3\text{/kmol}$$
$$\rho_V = \frac{M_V}{v_V} = \frac{105.27}{219.2} = 0.4802 \text{ kg/m}^3$$

Vapor molar enthalpy (datum = ideal gas at 298.15 K and 0 kPa): From (2-36) for ethylbenzene,

$$h^o_{\text{EB}_V} = -43098.9(350.65 - 298.15) + \left(\frac{707.151}{2}\right)(350.65^2 - 298.15^2) - \left(\frac{0.481063}{3}\right)(350.65^3 - 298.15^3) + \left(\frac{1.30084 \times 10^{-4}}{4}\right)(350.65^4 - 298.15^4)$$
$$= 7{,}351{,}900 \text{ J/kmol}$$

Similarly,

$$h^o_{\text{S}_V} = 6{,}957{,}700 \text{ J/kmol}$$

From (2), Table 2.4, for the mixture,

$$h_V = \sum y_i h^o_{iV} = (0.5559)(7{,}351{,}900) + (0.4441)(6{,}957{,}100) = 7{,}176{,}800 \text{ J/kmol}$$

Vapor molar entropy (datum = pure components as vapor at 298.15 K, 101.3 kPa): From (2-37), for each component,

$$\int_{T_0}^{T} \left(\frac{C^o_{P_V}}{T}\right) dT = 22{,}662 \text{ J/kmol-K} \quad \text{for ethylbenzene}$$
$$\text{and} \quad 21{,}450 \text{ J/kmol-K} \quad \text{for styrene}$$

From (3), Table 2.4, for the mixture,

$$s_V = [(0.5559)(22{,}662.4) + (0.4441)(21{,}450.3)] - 8{,}314 \ln\left(\frac{13.332}{101.3}\right) - 8{,}314[(0.5559)\ln(0.5559) + (0.4441)\ln(0.4441)] = 44{,}695 \text{ J/kmol-K}$$

Note that the terms for the pressure effect and the mixing effect are significant for this problem.

Liquid molar volume and density. From (2-38), for ethylbenzene,

$$\rho_{\text{EB}_L} = (289.8)(0.268)^{-(1-350.65/617.9)^{2/7}} = 816.9 \text{ kg/m}^3$$
$$v_{\text{EB}_L} = \frac{M_{\text{EB}}}{\rho_{\text{EB}_L}} = 0.1300 \text{ m}^3\text{/kmol}$$

Similarly,

$$\rho_{\text{S}_L} = 853.0 \text{ kg/m}^3$$
$$v_{\text{S}_L} = 0.1221 \text{ m}^3\text{/kmol}$$

From (4), Table 2.4, for the mixture,

$$v_L = (0.4848)(0.1300) + (0.5152)(0.1221) = 0.1259 \text{ m}^3\text{/kmol}$$
$$\rho_L = \frac{M_L}{v_L} = \frac{105.13}{0.1259} = 835.0 \text{ kg/m}^3$$

Liquid molar enthalpy (datum = ideal gas at 298.15 K): Use (5) in Table 2.4 for the mixture. For the enthalpy of vaporization of

ethylbenzene, from (2-41),

$$\Delta H_{\text{EB}}^{\text{vap}} = 8{,}314(350.65)^2\left[\frac{-(-7{,}440.61)}{(0+350.65)^2} + 0.00623121 + \frac{-(9.87052)}{(350.65)} + 6(4.13065\times10^{-18})(350.65)^5\right]$$
$$= 39{,}589{,}800 \text{ J/kmol}$$

Similarly,

$$\Delta H_{\text{S}}^{\text{vap}} = 40{,}886{,}700 \text{ J/kmol}$$

Then, applying (5), Table 2.4, using $h^o_{\text{EB}_V}$ and $h^o_{\text{S}_V}$ from above,

$$h_L = [(0.4848)(7{,}351{,}900 - 39{,}589{,}800) + (0.5152)(6{,}957{,}700 - 40{,}886{,}700)]$$
$$= -33{,}109{,}000 \text{ J/kmol}$$

Liquid molar entropy (datum = pure components as vapor at 298.15 K and 101.3 kPa): From (6), Table 2.4 for the mixture, using values for $\int_{T_0}^{T}(C^o_{P_V}/T)\,dT$ and ΔH^{vap} of EB and S from above,

$$s_L = (0.4848)\left(22{,}662 - \frac{39{,}589{,}800}{350.65}\right) + (0.5152)\left(21{,}450 - \frac{40{,}886{,}700}{350.65}\right) - 8.314\ln\left(\frac{13.332}{101.3}\right) - 8{,}314[0.4848\ln(0.4848) + 0.5152\ln(0.5152)]$$
$$= -70{,}150 \text{ J/kmol-K}$$

***K*-values:** Because (7), Table 2.4 will be used to compute the *K*-values, first estimate the vapor pressures using (2-39). For ethylbenzene,

$$\ln P^s_{\text{EB}} = 86.5008 + \left(\frac{-7{,}440.61}{(0+350.65}\right) + 0.00623121(350.65) + (-9.87052)\ln(350.65) + 4.13065\times10^{-18}(350.65)^6$$
$$= 9.63481$$
$$P^s_{\text{EB}} = \exp(9.63481) = 15{,}288 \text{ Pa} = 15.288 \text{ kPa}$$

Similarly,

$$P^s_{\text{S}} = 11.492 \text{ kPa}$$

From (7), Table 2.4,

$$K_{\text{EB}} = \frac{15.288}{13.332} = 1.147$$

$$K_{\text{S}} = \frac{11.492}{13.332} = 0.862$$

Relative volatility: From (2-21),

$$\alpha_{\text{EB,S}} = \frac{K_{\text{EB}}}{K_{\text{S}}} = \frac{1.147}{0.862} = 1.331$$

2.4 GRAPHICAL CORRELATIONS OF THERMODYNAMIC PROPERTIES

Calculations of estimated thermodynamic and other physical properties for the design of separation operations are most commonly carried out with computer-aided, process design

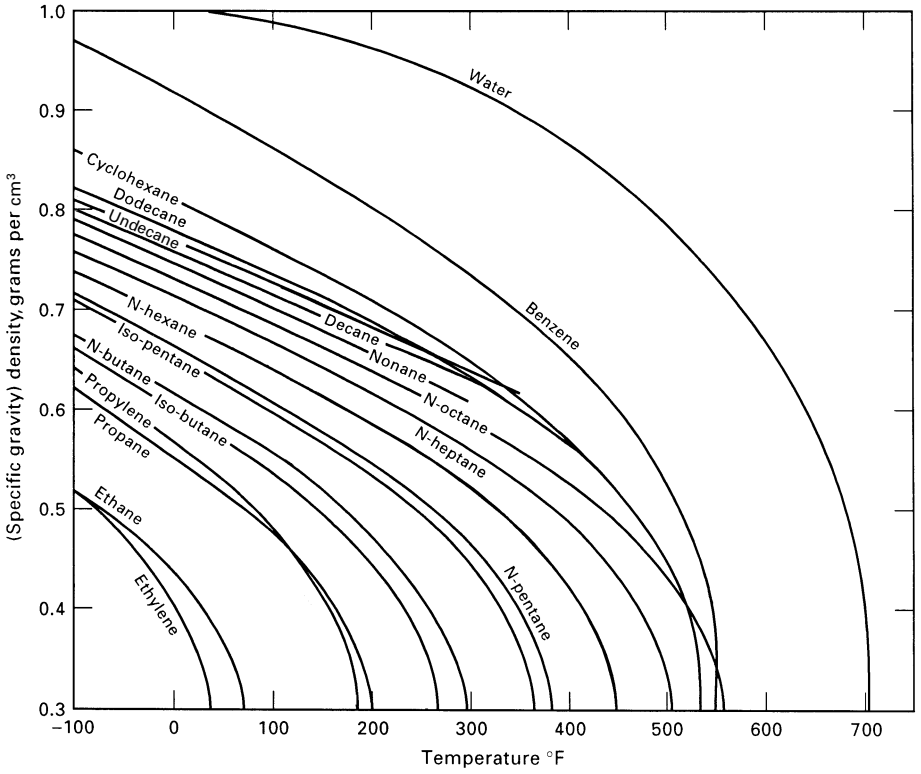

Figure 2.3 Hydrocarbon fluid densities.

[Adapted from G.G. Brown, D.L. Katz, G.G. Oberfell, and R.C. Alden, *Natural Gasoline and the Volatile Hydrocarbons,* Nat'l Gas Assoc. Amer., Tulsa, OK (1948).]

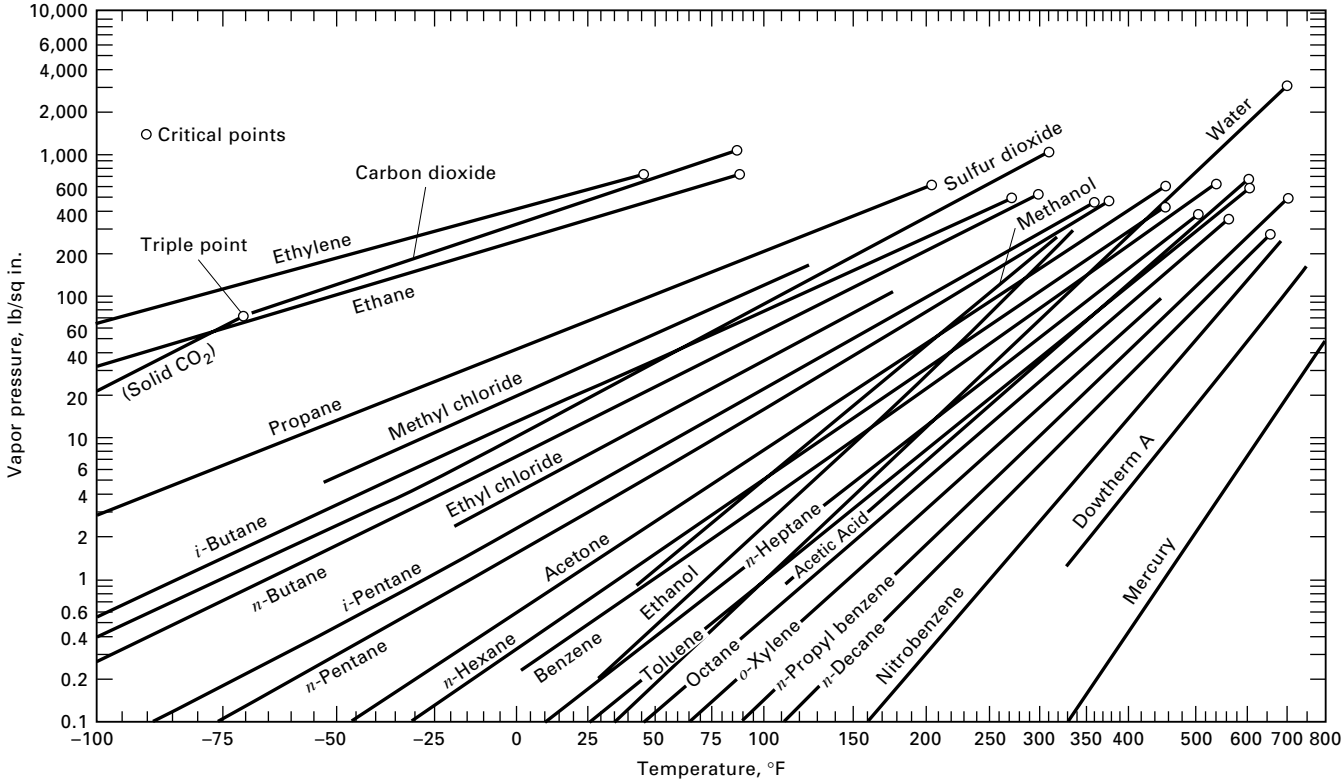

Figure 2.4 Vapor pressure as a function of temperature.

[Adapted from A.S. Faust, L.A. Wenzel, C.W. Clump, L. Maus, and L.B. Andersen, *Principles of Unit Operations,* John Wiley and Sons, New York (1960).]

and simulation programs, such as Aspen Plus, HYSYS, ChemCad, and Pro/II. However, plots of properties can best show effects of temperature and pressure. Some representative plots, which are readily generated by simulation programs, are shown in this section.

Saturated liquid densities as a function of temperature are plotted for some hydrocarbons in Figure 2.3. The density decreases rapidly as the critical temperature is approached until it becomes equal to the density of the vapor phase at the critical point. The liquid density curves are well correlated by the modified Rackett equation (2-38).

Figure 2.4 is a plot of liquid-state vapor pressures for some common chemicals, covering a wide range of temperature from below the normal boiling point to the critical temperature, where the vapor pressure terminates at the critical pressure. In general, the curves are found to fit the extended Antoine equation (2-39) reasonably well. This plot is useful for determining the phase state (liquid or vapor) of a pure substance and for estimating Raoult's law *K*-values from (2-44) [or (3) in Table 2.3].

Curves of ideal-gas, zero-pressure enthalpy over a wide range of temperature are given in Figure 2.5 for light-paraffin hydrocarbons. The datum is the liquid phase at 0°C, at which the enthalpy is zero. The derivatives of these curves fit the fourth-degree polynomial (2-35) for the ideal-gas heat

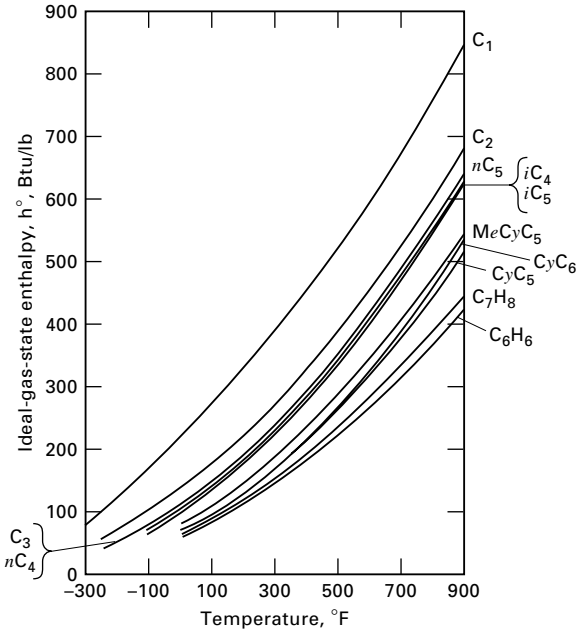

Figure 2.5 Ideal-gas-state enthalpy of pure components.

[Adapted from *Engineering Data Book,* 9th ed., Gas Processors Suppliers Association, Tulsa (1972).]

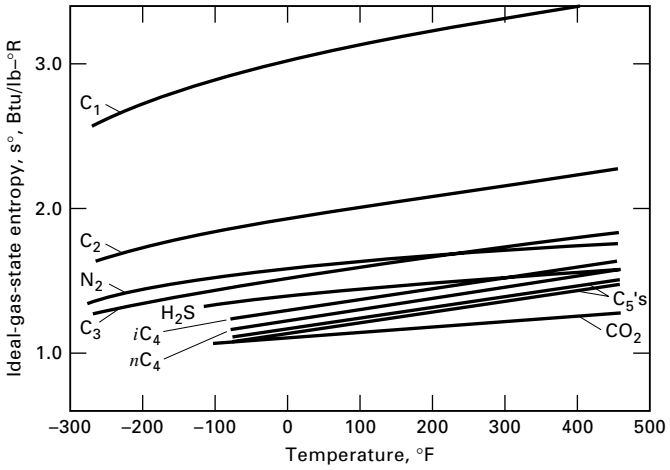

Figure 2.6 Ideal-gas-state entropy of pure components.
[Adapted from *Engineering Data Book,* 9th ed., Gas Processors Suppliers Association, Tulsa (1972).]

capacity reasonably well. Curves of ideal-gas entropy of several light gases, over a wide range of temperature, are given in Figure 2.6.

Enthalpies (heats) of vaporization are plotted as a function of saturation temperature in Figure 2.7 for light-paraffin hydrocarbons. These values are independent of pressure and decrease to zero at the critical point, where vapor and liquid phases become indistinguishable.

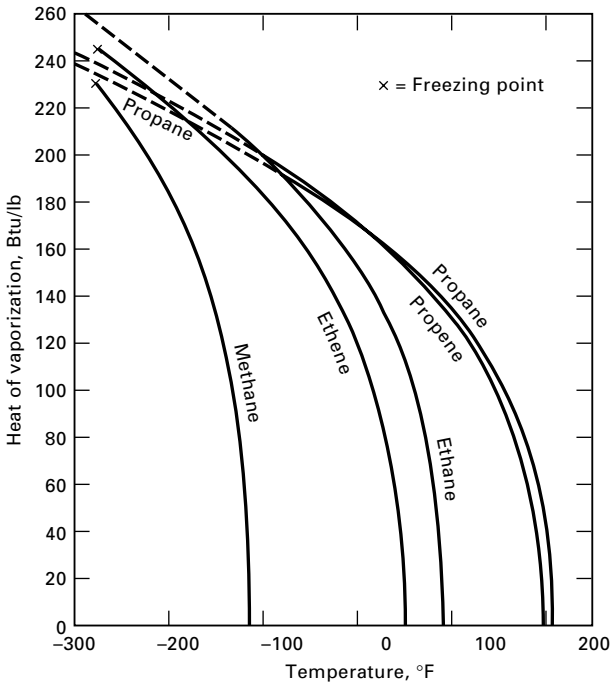

Figure 2.7 Heat of vaporization of light olefins and paraffins.
[Adapted from American Petroleum Institute, Technical Data Book, Washington, DC (Aug. 1963).]

Nomographs for determining the effects of temperature and pressure on the *K*-values of hydrocarbons and light gases are presented in Figures 2.8 and 2.9, which are taken from Hadden and Grayson [15]. In both charts, all *K*-values collapse to 1.0 at a pressure of 5,000 psia (34.5 MPa). This pressure, called the *convergence pressure,* depends on the boiling range of the components in the mixture. For example, in Figure 2.10 the components of the mixture (N_2 to nC_{10}) cover a very wide boiling-point range, resulting in a convergence pressure of close to 2,500 psia. For narrow-boiling mixtures, such as a mixture of ethane and propane, the convergence pressure is generally less than 1,000 psia. The *K*-value charts of Figures 2.8 and 2.9 apply strictly to a convergence pressure of 5,000 psia. A detailed procedure for correcting for the convergence pressure is given by Hadden and Grayson [15]. Use of the nomographs is illustrated below in Exercise 2.4.

No simple charts are available for estimating liquid–liquid equilibrium constants (distribution coefficients) because of the pronounced effect of composition. However, for ternary systems that are dilute in the solute and involve almost immiscible solvents, an extensive tabulation of distribution coefficients for the solute is given by Robbins [16].

EXAMPLE 2.4

Petroleum refining begins with the distillation, at near-atmospheric pressure, of crude oil into fractions of different boiling ranges. The fraction boiling from 0 to 100°C, the light naphtha, is a blending stock for gasoline. The fraction boiling from 100 to 200°C, the heavy naphtha, undergoes subsequent chemical processing into more useful products. One such process is steam cracking to produce a gas containing ethylene, propylene, and a number of other compounds, including benzene and toluene. This gas is then sent to a distillation train to separate the mixture into a dozen or more products. In the first column, hydrogen and methane are removed by cryogenic distillation at 3.2 MPa (464 psia). At a tray in the distillation column where the temperature is 40°F, use the appropriate *K*-value nomograph to estimate *K*-values for H_2, CH_4, C_2H_4, and C_3H_6.

SOLUTION

At 40°F, Figure 2.8 applies. The *K*-value of hydrogen depends on the other compounds in the mixture. Because appreciable amounts of benzene and toluene are present, locate a point (call it A) midway between the points for "H_2 in benzene" and "H_2 in toluene." Next, locate a point (call it B) at 40°F and 464 psia on the T–P grid. Connect points A and B with a straight line and read a value of $K = 100$ where the line intersects the *K* scale.

In a similar way, with the same location for point B, read $K = 11$ for methane. For ethylene (ethene) and propylene (propene), the point A is located on the normal boiling-point scale and the same point is used for B. Resulting *K*-values are 1.5 and 0.32, respectively.

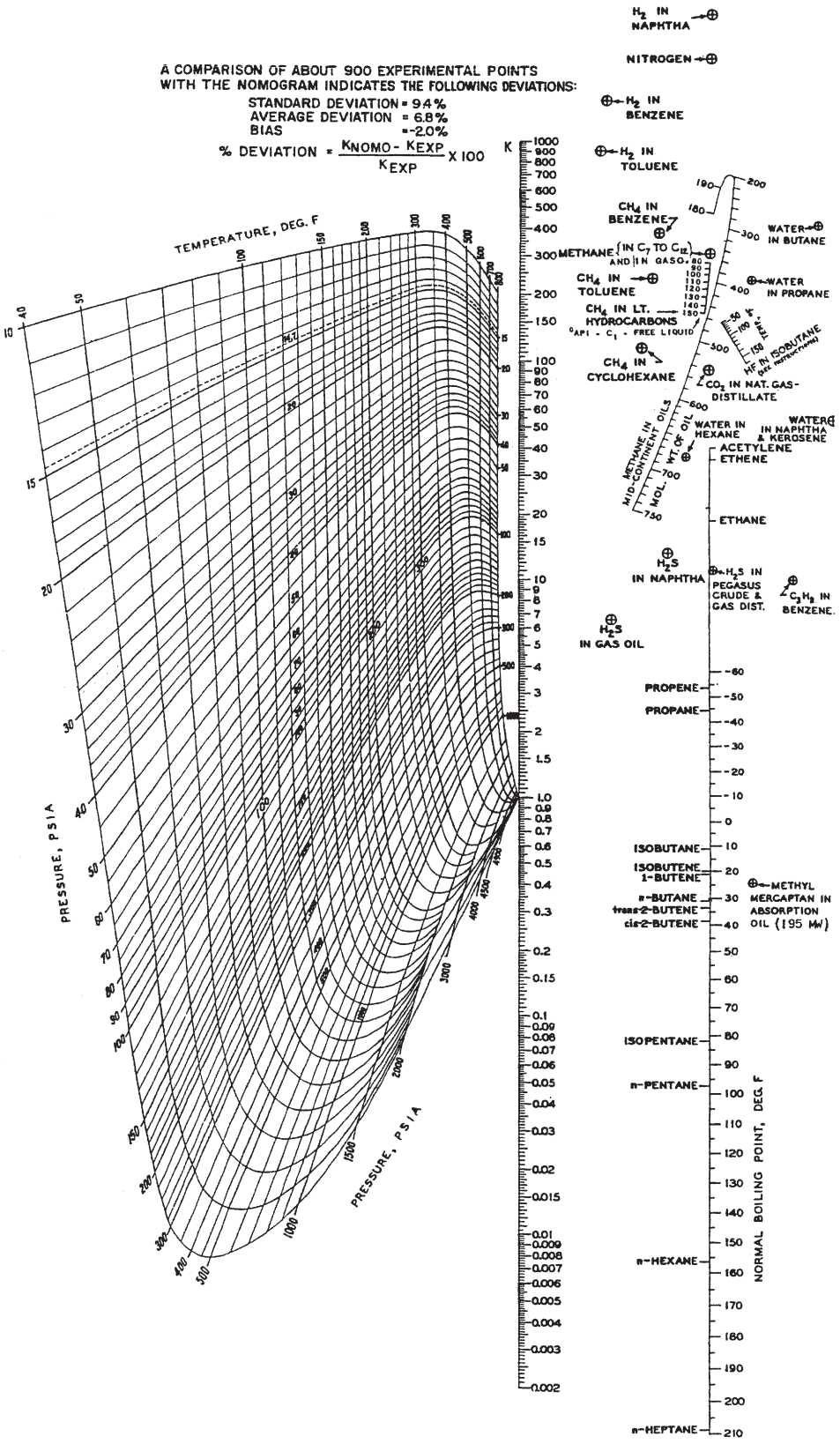

Figure 2.8 Vapor–liquid equilibria, 40 to 800°F.

[From S.T. Hadden and H.G. Grayson, *Hydrocarbon Proc. and Petrol. Refiner,* **40,** 207 (Sept. 1961), with permission.]

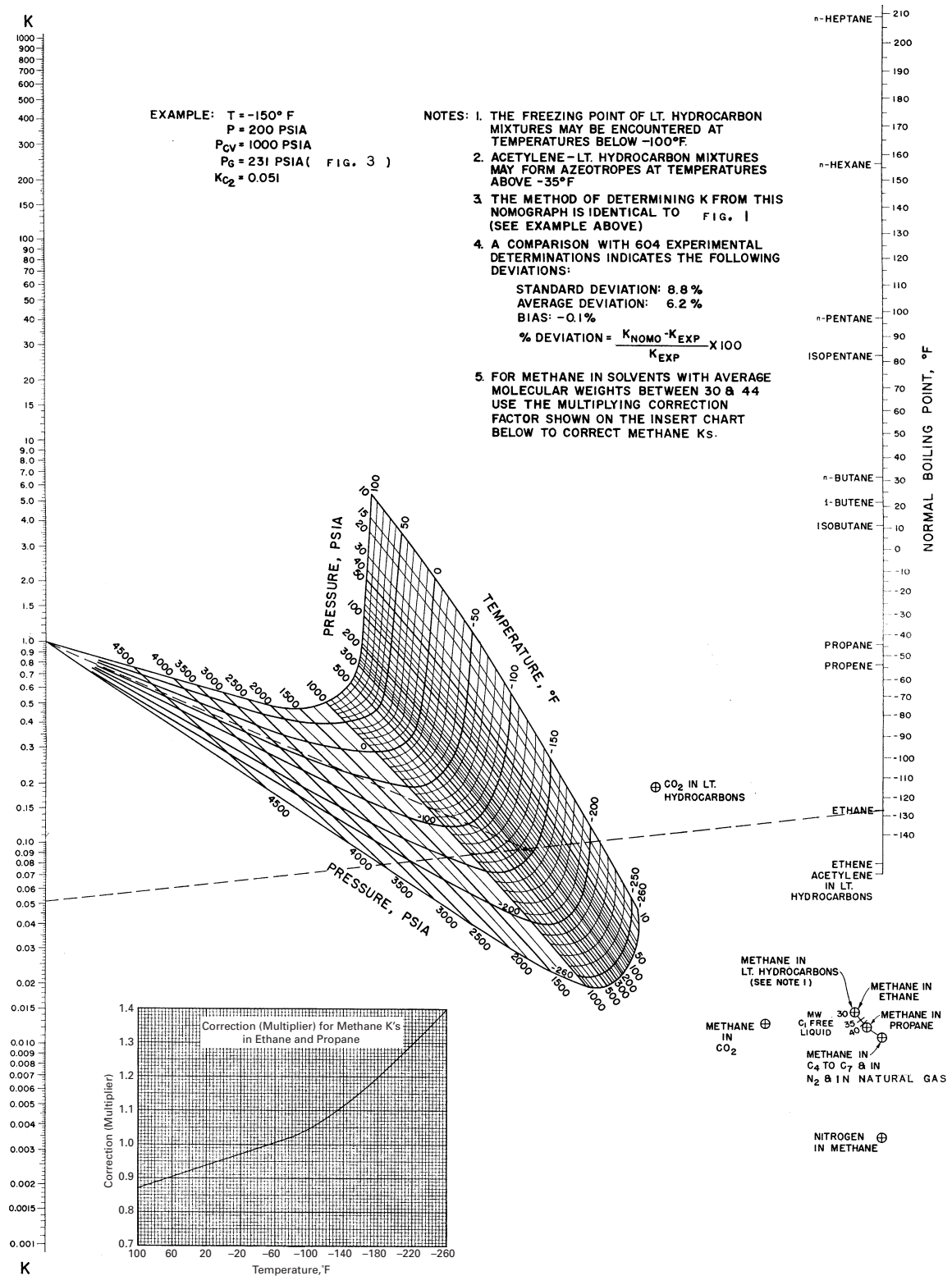

Figure 2.9 Vapor–liquid equilibria, –260 to 100°F.

[From S.T. Hadden and H.G. Grayson, *Hydrocarbon Proc. and Petrol. Refiner,* **40,** 207 (Sept. 1961), with permission.]

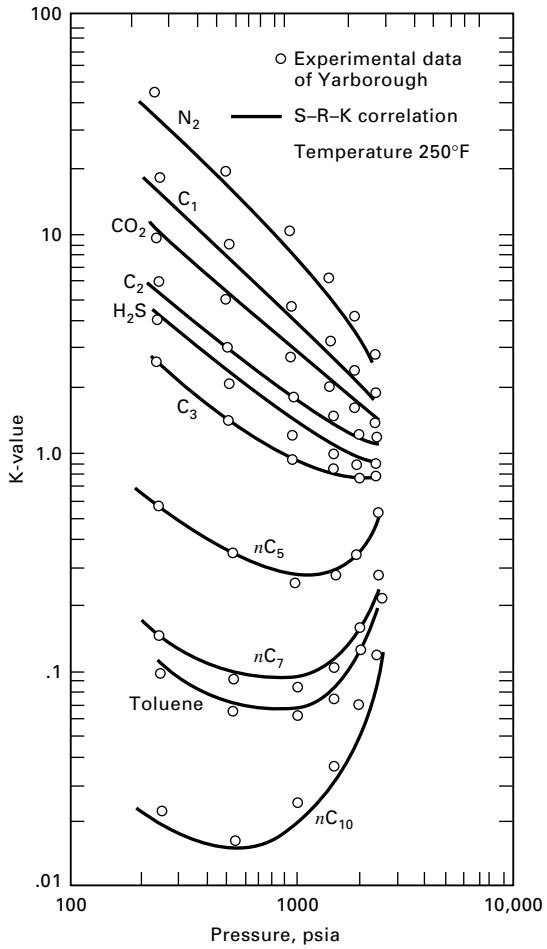

Figure 2.10 Comparison of experimental *K*-value data and S–R–K correlation.

2.5 NONIDEAL THERMODYNAMIC PROPERTY MODELS

Unlike the equations of Table 2.1, which are universally applicable to all pure substances and mixtures, whether ideal or nonideal, no universal equations are available for computing, for nonideal mixtures, values of thermodynamic properties such as density, enthalpy, entropy, fugacities, and activity coefficients as functions of temperature, pressure, and phase composition. Instead, two types of models are used: (1) *P–v–T* equation-of-state models and (2) activity coefficient or free-energy models. These are based on *constitutive equations* because they depend on the constitution or nature of the components in the mixture.

P–v–T Equation-of-State Models

The first type of model is a relationship between molar volume (or density), temperature, and pressure, usually referred to as a *P–v–T* equation of state. A large number of such equations have been proposed, mostly for the vapor phase. The simplest is the ideal-gas law, which applies only at low pressures or high temperatures because it neglects the volume occupied by the molecules and intermolecular forces among the molecules. All other equations of state attempt to correct for these two deficiencies. The equations of state that are most widely used by chemical engineers are listed in Table 2.5. These and other equations of state are discussed in some detail by Poling et al. [11].

Not included in Table 2.5 is the van der Waals equation, $P = RT/(v-b) - a/v^2$, where a and b are species-dependent constants that can be estimated from the critical temperature and pressure. The van der Waals equation was the first successful approach to the formulation of an equation of state for a nonideal gas. It is rarely used by chemical

Table 2.5 Useful Equations of State

Name	Equation	Equation Constants and Functions
(1) Ideal gas law	$P = \dfrac{RT}{v}$	None
(2) Generalized	$P = \dfrac{ZRT}{v}$	$Z = Z\{P_r, T_r, Z_c \text{ or } \omega\}$ as derived from data
(3) Redlich–Kwong (R–K)	$P = \dfrac{RT}{v-b} - \dfrac{a}{v^2+bv}$	$b = 0.08664RT_c/P_c$ $a = 0.42748R^2T_c^{2.5}/P_cT^{0.5}$
(4) Soave–Redlich–Kwong (S–R–K or R–K–S)	$P = \dfrac{RT}{v-b} - \dfrac{a}{v^2+bv}$	$b = 0.08664RT_c/P_c$ $a = 0.42748R^2T_c^2\left[1+f_\omega\left(1-T_r^{0.5}\right)\right]^2/P_c$ $f_\omega = 0.48 + 1.574\omega - 0.176\omega^2$
(5) Peng–Robinson (P–R)	$P = \dfrac{RT}{v-b} - \dfrac{a}{v^2+2bv-b^2}$	$b = 0.07780RT_c/P_c$ $a = 0.45724R^2T_c^2\left[1+f_\omega\left(1-T_r^{0.5}\right)\right]^2/P_c$ $f_\omega = 0.37464 + 1.54226\omega - 0.26992\omega^2$

engineers because its range of application is too narrow. However, its development did suggest that all species might have equal reduced molar volumes, $v_r = v/v_c$, at the same reduced temperature, $T_r = T/T_c$, and reduced pressure, $P_r = P/P_c$. This finding, referred to as the *law* (*principle* or *theorem*) *of corresponding states,* was utilized to develop the generalized equation of state given as (2) in Table 2.5. That equation defines the *compressibility factor, Z*, which is a function of P_r, T_r, and the critical compressibility factor, Z_c, or the *acentric factor,* ω, which is determined from experimental P–v–T data. The acentric factor, introduced by Pitzer et al. [17], accounts for differences in molecular shape and is determined from the vapor pressure curve:

$$\omega = \left[-\log\left(\frac{P^s}{P_c}\right)_{T_r=0.7} \right] - 1.000 \qquad (2\text{-}45)$$

This definition results in a value for ω of zero for symmetric molecules. Some typical values of ω are 0.264, 0.490, and 0.649 for toluene, *n*-decane, and ethyl alcohol, respectively, as taken from the extensive tabulation of Poling et al. [11].

In 1949, Redlich and Kwong [18] published an equation of state that, like the van der Waals equation, contains only two constants, both of which can be determined from T_c and P_c, by applying the critical conditions

$$\left(\frac{\partial P}{\partial v}\right)_{T_c} = 0 \qquad \text{and} \qquad \left(\frac{\partial^2 P}{\partial v^2}\right)_{T_c} = 0$$

However, the R–K equation, given as (3) in Table 2.5, is a considerable improvement over the van der Waals equation. A study by Shah and Thodos [19] showed that the simple R–K equation, when applied to nonpolar compounds, has an accuracy that compares quite favorably with equations containing many more constants. Furthermore, the R–K equation can approximate the liquid-phase region.

If the R–K equation is expanded to obtain a common denominator, a cubic equation in v results. Alternatively, (2) and (3) in Table 2.5 can be combined to eliminate v to give the compressibility factor, Z, form of the R–K equation:

$$Z^3 - Z^2 + (A - B - B^2)Z - AB = 0 \qquad (2\text{-}46)$$

where

$$A = \frac{aP}{R^2T^2} \qquad (2\text{-}47)$$

$$B = \frac{bP}{RT} \qquad (2\text{-}48)$$

Equation (2-46), which is cubic in Z, can be solved analytically for three roots (e.g., see *Perry's Handbook,* 7th ed., p. 4-20). In general, at supercritical temperatures, where only one phase can exist, one real root and a complex conjugate pair of roots are obtained. Below the critical temperature, where vapor and/or liquid phases can exist, three real roots are obtained, with the largest value of Z (largest v) corresponding to the vapor phase—that is, Z_V—and the smallest Z (smallest v) corresponding to the liquid phase—that is, Z_L. The intermediate value of Z is of no practical use.

To apply the R–K equation to mixtures, *mixing rules* are used to average the constants a and b for each component in the mixture. The recommended rules for vapor mixtures of C components are

$$a = \sum_{i=1}^{C}\left[\sum_{j=1}^{C} y_i y_j (a_i a_j)^{0.5}\right] \qquad (2\text{-}49)$$

$$b = \sum_{i=1}^{C} y_i b_i \qquad (2\text{-}50)$$

EXAMPLE 2.5

Glanville, Sage, and Lacey [20] measured specific volumes of vapor and liquid mixtures of propane and benzene over wide ranges of temperature and pressure. Use the R–K equation to estimate specific volume of a vapor mixture containing 26.92 wt% propane at 400°F (477.6 K) and a saturation pressure of 410.3 psia (2,829 kPa). Compare the estimated and experimental values.

SOLUTION

Let propane be denoted by P and benzene by B. The mole fractions are

$$y_P = \frac{0.2692/44.097}{(0.2692/44.097) + (0.7308/78.114)} = 0.3949$$

$$y_B = 1 - 0.3949 = 0.6051$$

The critical constants for propane and benzene are given by Poling et al. [11]:

	Propane	Benzene
T_c, K	369.8	562.2
P_c, kPa	4,250	4,890

From the equations for the constants b and a in Table 2.5 for the R–K equation, using SI units,

$$b_P = \frac{0.08664(8.3144)(369.8)}{4{,}250} = 0.06268 \text{ m}^3/\text{kmol}$$

$$a_P = \frac{0.42748(8.3144)^2(369.8)^{2.5}}{(4{,}250)(477.59)^{0.5}}$$

$$= 836.7 \text{ kPa-m}^6/\text{kmol}^2$$

Similarly,

$$b_B = 0.08263 \text{ m}^3/\text{kmol}$$

$$a_B = 2{,}072 \text{ kPa-m}^6/\text{kmol}^2$$

From (2-50),

$$b = (0.3949)(0.06268) + (0.6051)(0.08263) = 0.07475 \text{ m}^3/\text{kmol}$$

From (2-49),

$$a = y_P^2 a_P + 2y_P y_B (a_P a_B)^{0.5} + y_B^2 a_B$$
$$= (0.3949)^2(836.7) + 2(0.3949)(0.6051)[(836.7)(2{,}072)]^{0.5}$$
$$+ (0.6051)^2(2{,}072) = 1{,}518 \text{ kPa-m}^6/\text{kmol}^2$$

From (2-47) and (2-48) using SI units,

$$A = \frac{(1{,}518)(2{,}829)}{(8.314)^2(477.59)^2} = 0.2724$$

$$B = \frac{(0.07475)(2{,}829)}{(8.314)(477.59)} = 0.05326$$

From (2-46), we obtain the cubic Z form of the R–K equation:

$$Z^3 - Z^2 + 0.2163Z - 0.01451 = 0$$

Solving this equation gives one real root and a conjugate pair of complex roots:

$$Z = 0.7314, \quad 0.1314 + 0.04243i, \quad 0.1314 - 0.04243i$$

The one real root is assumed to be that for the vapor phase.

From (2) of Table 2.5, the molar volume is

$$v = \frac{ZRT}{P} = \frac{(0.7314)(8.314)(477.59)}{2{,}829} = 1.027 \text{ m}^3/\text{kmol}$$

The average molecular weight of the mixture is computed to 64.68 kg/kmol. The specific volume is

$$\frac{v}{M} = \frac{1.027}{64.68} = 0.01588 \text{ m}^3/\text{kg} = 0.2543 \text{ ft}^3/\text{lb}$$

Glanville et al. report experimental values of $Z = 0.7128$ and $v/M = 0.2478$ ft^3/lb, which are within 3% of the above estimated values.

Following the success of earlier work by Wilson [21], Soave [6] added a third parameter, the acentric factor, ω, defined by (2-45), to the R–K equation. The resulting, so-called Soave–Redlich–Kwong (S–R–K) or Redlich–Kwong–Soave (R–K–S) equation of state, given as (4) in Table 2.5, was immediately accepted for application to mixtures containing hydrocarbons and/or light gases because of its simplicity and accuracy. The main improvement was to make the parameter a a function of the acentric factor and temperature so as to achieve a good fit to vapor pressure data of hydrocarbons and thereby greatly improve the ability of the equation to predict properties of the liquid phase.

Four years after the introduction of the S–R–K equation, Peng and Robinson [7] presented a further modification of the R–K and S–R–K equations in an attempt to achieve improved agreement with experimental data in the critical region and for liquid molar volume. The Peng–Robinson (P–R) equation of state is listed as (5) in Table 2.5. The S–R–K and P–R equations of state are widely applied in process calculations, particularly for saturated vapors and liquids. When applied to mixtures of hydrocarbons and/or light gases, the mixing rules are given by (2-49) and (2-50), except that (2-49) is often modified to include a binary interaction coefficient, k_{ij}:

$$a = \sum_{i=1}^{C} \left[\sum_{j=1}^{C} y_i y_j (a_i a_j)^{0.5} (1 - k_{ij}) \right] \qquad (2\text{-}51)$$

Values of k_{ij}, back-calculated from experimental data, have been published for both the S–R–K and P–R equations. Knapp et al. [22] present an extensive tabulation. Generally, k_{ij} is taken as zero for hydrocarbons paired with hydrogen or other hydrocarbons.

Although the S–R–K and P–R equations were not intended to be applied to mixtures containing polar organic compounds, they are finding increasing use in such applications by employing large values of k_{ij}, in the vicinity of 0.5, as back-calculated from experimental data. However, a preferred procedure for mixtures containing polar organic compounds is to use a more theoretically based mixing rule such as that of Wong and Sandler, which is discussed in detail in Chapter 11 and which bridges the gap between a cubic equation of state and an activity-coefficient equation.

Another theoretical basis for polar and nonpolar substances is the virial equation of state due to Thiesen [23] and Onnes [24]. A common representation of the virial equation, which can be derived from the statistical mechanics of the forces between the molecules, is a power series in $1/v$ for Z:

$$Z = 1 + \frac{B}{v} + \frac{C}{v^2} + \cdots \qquad (2\text{-}52)$$

An empirical modification of the virial equation is the Starling form [5] of the Benedict–Webb–Rubin (B–W–R) equation of state for hydrocarbons and light gases in both the gas and liquid phases. Walas [25] presents an extensive discussion of B–W–R-type equations, which because of the large number of terms and species constants (at least 8), is not widely used except for pure substances at cryogenic temperatures. A more useful modification of the B–W–R equation is a generalized corresponding-states form developed by Lee and Kesler [26] with an important extension to mixtures by Plöcker et al. [8]. All of the constants in the L–K–P equation are given in terms of the acentric factor and reduced temperature and pressure, as developed from P–v–T data for three simple fluids (ω = 0), methane, argon, and krypton, and a reference fluid (ω = 0.398), n-octane. The equations, constants, and mixing rules in terms of pseudo-critical properties are given by Walas [25]. The Lee–Kesler–Plöcker (L–K–P) equation of state describes vapor and liquid mixtures of hydrocarbons and/or light gases over wide ranges of temperature and pressure.

Derived Thermodynamic Properties from *P–v–T* Models

In the previous subsection, several useful P–v–T equations of state for the estimation of the molar volume (or density) or pure substances and mixtures in either the vapor or liquid phase were presented. If a temperature-dependent, ideal-gas heat capacity or enthalpy equation, such as (2-35) or (2-36), is also available, all other vapor- and liquid-phase properties can be derived in a consistent manner by applying the classical integral equations of thermodynamics given in Table 2.6. These equations, in the form of departure (from the ideal gas) equations of Table 2.4, and often referred to as residuals, are applicable to vapor or liquid phases.

Table 2.6 Classical Integral Departure Equations of Thermodynamics

At a given temperature and composition, the following equations give the effect of pressure above that for an ideal gas.

Mixture enthalpy:

$$(1)\ \left(h - h_V^o\right) = Pv - RT - \int_\infty^v \left[P - T\left(\frac{\partial P}{\partial T}\right)_v\right] dv$$

Mixture entropy:

$$(2)\ \left(s - s_V^o\right) = \int_\infty^v \left(\frac{\partial P}{\partial T}\right)_v dv - \int_\infty^v \frac{R}{v}\, dv$$

Pure-component fugacity coefficient:

$$(3)\ \phi_{iV} = \exp\left[\frac{1}{RT}\int_0^P \left(v - \frac{RT}{P}\right) dP\right]$$

$$= \exp\left[\frac{1}{RT}\int_v^\infty \left(P - \frac{RT}{v}\right) dv - \ln Z + (Z-1)\right]$$

Partial fugacity coefficient:

$$(4)\ \bar{\phi}_{iV} = \exp\left\{\frac{1}{RT}\int_V^\infty \left[\left(\frac{\partial P}{\partial N_i}\right)_{T,V,N_j} - \frac{RT}{V}\right] dV - \ln Z\right\}$$

where $V = v\sum_{i=1}^{C} N_i$

When the ideal-gas law, $P = RT/v$, is substituted into (1) to (4) of Table 2.6, the results for the vapor, as expected, are

$$\left(h - h_V^o\right) = 0 \qquad \phi = 1$$
$$\left(s - s_V^o\right) = 0 \qquad \bar{\phi} = 1$$

However, when the R–K equation is substituted into the equations of Table 2.6, the following results for the vapor phase are obtained after a rather tedious exercise in calculus:

$$h_V = \sum_{i=1}^{C}(y_i h_{iV}^o) + RT\left[Z_V - 1 - \frac{3A}{2B}\ln\left(1 + \frac{B}{Z_V}\right)\right] \tag{2-53}$$

$$s_V = \sum_{i=1}^{C}(y_i s_{iV}^o) - R\ \ln\left(\frac{P}{P^o}\right) - R\sum_{i=1}^{C}(y_i \ln\ y_i) + R\ \ln(Z_V - B) \tag{2-54}$$

$$\phi_V = \exp\left[Z_V - 1 - \ln(Z_V - B) - \frac{A}{B}\ln\left(1 + \frac{B}{Z_V}\right)\right] \tag{2-55}$$

$$\bar{\phi}_{iV} = \exp\left[(Z_V - 1)\frac{B_i}{B} - \ln(Z_V - B) - \frac{A}{B}\left(2\sqrt{\frac{A_i}{A}} - \frac{B_i}{B}\right)\ln\left(1 + \frac{B}{Z_V}\right)\right] \tag{2-56}$$

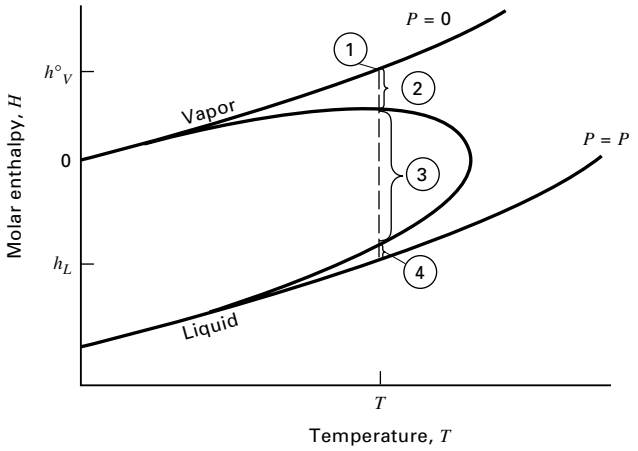

Figure 2.11 Contributions to enthalpy.

The results for the liquid phase are identical if y_i and Z_V (but not h_{iV}^o) are replaced by x_i and Z_L, respectively. It may be surprising that the liquid-phase forms of (2-53) and (2-54) account for the enthalpy and entropy of vaporization, respectively. This is because the R–K equation of state, as well as the S–R–K and P–R equations, are continuous functions in passing between the vapor and liquid regions, as shown for enthalpy in Figure 2.11. Thus, the liquid enthalpy is determined by accounting for the following four effects for a pure species at a temperature below the critical. From (1), Table 2.6, the four contributions to enthalpy in Figure 2.11 are as follows:

$$h_L = h_V^o + Pv - RT - \int_\infty^v \left[P - T\left(\frac{\partial P}{\partial T}\right)_v\right] dv$$

$$= \underbrace{h_V^o}_{\text{(1) Vapor at zero pressure}}$$

$$+ \underbrace{(Pv)_{V_s} - RT - \int_\infty^{v_{V_s}} \left[P - T\left(\frac{\partial P}{\partial T}\right)_v\right] dv}_{\text{(2) Pressure correction for vapor to saturation pressure}}$$

$$\underbrace{- T\left(\frac{\partial P}{\partial T}\right)_s (v_{V_s} - v_{L_s})}_{\text{(3) Latent heat of vaporization}}$$

$$\underbrace{+[(Pv)_L - (Pv)_{L_s}] - \int_{v_{L_s}}^{v_L} \left[P - T\left(\frac{\partial P}{\partial T}\right)_v\right] dv}_{\text{(4) Correction to liquid for pressure in excess of saturation pressure}} \tag{2-57}$$

where the subscript s refers to the saturation pressure.

The fugacity coefficient, ϕ, of a pure species at temperature T and pressure P from the R–K equation, as given by (2-55), applies to the vapor for $P < P_i^s$. For $P > P_i^s$, ϕ is the fugacity coefficient of the liquid. Saturation pressure corresponds to the condition of $\phi_V = \phi_L$. Thus, at a temperature $T < T_c$, the saturation pressure (vapor pressure), P^s, can be estimated from the R–K equation of state by setting (2-55) for the vapor equal to (2-55) for the liquid and solving, by an iterative procedure, for P, which then equals P^s.

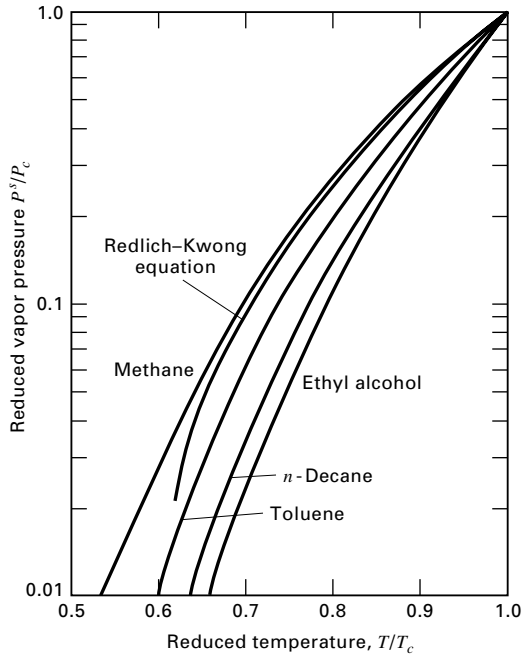

Figure 2.12 Reduced vapor pressure.

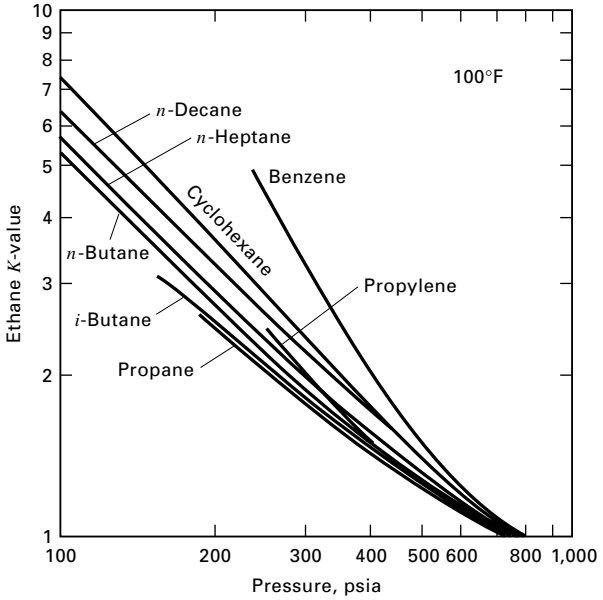

Figure 2.13 K-values of ethane in binary hydrocarbon mixtures at 100°F.

The results, as given by Edmister [27], are plotted in reduced form in Figure 2.12. The R–K vapor-pressure curve does not satisfactorily represent data for a wide range of molecular shapes, as witnessed by the experimental curves for methane, toluene, *n*-decane, and ethyl alcohol on the same plot. This failure represents one of the major shortcomings of the R–K equation and is the main reason why Soave [6] modified the R–K equation by introducing the acentric factor in such a way as to greatly improve agreement with experimental vapor-pressure data. Thus, while the critical constants, T_c and P_c alone are insufficient to generalize thermodynamic behavior, a substantial improvement is made by incorporating into the P–v–T equation a third parameter that represents the generic differences in the reduced-vapor-pressure curves.

As seen in (2-56), partial fugacity coefficients depend on pure-species properties, A_i and B_i, and mixture properties, A and B. Once $\bar{\phi}_{iV}$ and $\bar{\phi}_{iL}$ are computed from (2-56), a K-value can be estimated from (2-26).

The most widely used P–v–T equations of state for separation calculations involving vapor and liquid phases are the S–R–K, P–R, and L–K–P relations. These equations are combined with the integral departure equations of Table 2.6 to obtain useful equations for estimating the enthalpy, entropy, fugacity coefficients, partial fugacity coefficients of vapor and liquid phases, and K-values. The results of the integrations are even more complex than (2-53) to (2-56) and are unsuitable for manual calculations. However, computer programs for making calculations with these equations are rapid, accurate, and readily available. Such programs are incorporated into widely used steady-state, computer-aided process design and simulation programs, such as Aspen Plus, HYSYS, ChemCad, and Pro/II.

Ideal K-values as determined from Eq. (7) in Table 2.4, depend only on temperature and pressure, and not on composition. Most frequently, ideal K-values are applied to mixtures of nonpolar compounds, particularly hydrocarbons such as paraffins and olefins. Figure 2.13 shows experimental K-value curves for a light hydrocarbon, ethane, in various binary mixtures with other, less volatile hydrocarbons at 100°F (310.93 K) for pressures from 100 psia (689.5 kPa) to *convergence pressures* between 720 and 780 psia (4.964 MPa to 5.378 MPa). At the convergence pressure, separation by operations involving vapor–liquid equilibrium becomes impossible because all K-values become 1.0. The temperature of 100°F is close to the critical temperature of 550°R (305.6 K) for ethane. Figure 2.13 shows that ethane does not form ideal solutions at 100°F with all the other components because the K-values depend on the other component, even for paraffin homologs. For example, at 300 psia, the K-value of ethane in benzene is 80% higher than in propane.

The ability of equations of state, such as S–R–K, P–R, and L–K–P equations, to predict the effect of composition as well as the effect of temperature and pressure on K-values of multicomponent mixtures of hydrocarbons and light gases is shown in Figure 2.10. The mixture contains 10 species ranging in volatility from nitrogen to *n*-decane. The experimental data points, covering almost a 10-fold range of pressure at 250°F, are those of Yarborough [28]. Agreement with the S–R–K equation is very good.

EXAMPLE 2.6

In the high-pressure, high-temperature, thermal hydrodealkylation of toluene to benzene ($C_7H_8 + H_2 \rightarrow C_6H_6 + CH_4$), excess hydrogen is used to minimize cracking of aromatics to light gases. In practice, conversion of toluene per pass through the reactor is only 70%. To separate and recycle hydrogen, hot reactor effluent vapor of 5,597 kmol/h at 500 psia (3,448 kPa) and 275°F (408.2 K) is partially condensed to 120°F (322 K), with product phases separated in a flash drum. If the composition of the reactor effluent is as follows, and the flash drum pressure is 485 psia (3,344 kPa), calculate equilibrium compositions and flow rates of vapor and liquid leaving the flash drum and the amount of heat that must be transferred using a computer-aided, steady-state, simulation program with each of the equation-of-state models discussed above. Compare the results, including flash-drum *K*-values and enthalpy and entropy changes.

Component	Mole Fraction
Hydrogen (H)	0.3177
Methane (M)	0.5894
Benzene (B)	0.0715
Toluene (T)	0.0214
	1.0000

SOLUTION

The computations were made with a computer-aided, process-simulation program, using the S–R–K, P–R, and L–K–P equations of state. The results at 120°F and 485 psia are as follows:

	Equation of State		
	S–R–K	P–R	L–K–P
Vapor flows, kmol/h:			
Hydrogen	1,777.1	1,774.9	1,777.8
Methane	3,271.0	3,278.5	3,281.4
Benzene	55.1	61.9	56.0
Toluene	6.4	7.4	7.0
Total	5,109.6	5,122.7	5,122.2
Liquid flows, kmol/h:			
Hydrogen	1.0	3.3	0.4
Methane	27.9	20.4	17.5
Benzene	345.1	338.2	344.1
Toluene	113.4	112.4	112.8
Total	487.4	474.3	474.8
K-values:			
Hydrogen	164.95	50.50	466.45
Methane	11.19	14.88	17.40
Benzene	0.01524	0.01695	0.01507
Toluene	0.00537	0.00610	0.00575
Enthalpy change, GJ/h	35.267	34.592	35.173
Entropy change, MJ/h-K	−95.2559	−93.4262	−95.0287
Percent of benzene and toluene condensed	88.2	86.7	87.9

Because the reactor effluent is mostly hydrogen and methane, the effluent at 275°F and 500 psia, and the equilibrium vapor at 120°F and 485 psia are nearly ideal gases ($0.98 < Z < 1.00$), despite the moderately high pressures. Thus, the enthalpy and entropy changes are dominated by vapor heat capacity and latent heat effects, which are largely independent of which equation of state is used. Consequently, the enthalpy and entropy changes among the three equations of state differ by less than 2%.

Significant differences exist for the *K*-values of H_2 and CH_4. However, because the values are in all cases large, the effect on the amount of equilibrium vapor is very small. Reasonable *K*-values for H_2 and CH_4, based on experimental data, are 100 and 13, respectively. *K*-values for benzene and toluene differ among the three equations of state by as much as 11% and 14%, respectively, which, however, causes less than a 2% difference in the percentage of benzene and toluene condensed. Raoult's law *K*-values for benzene and toluene, based on vapor-pressure data, are 0.01032 and 0.00350, which are considerably lower than the values computed from each of the three equations of state because deviations to fugacities due to pressure are important in the liquid phase and, particularly, in the vapor phase.

Note that the material balances are precisely satisfied for each equation of state. However, the user of a computer-aided design and simulation program should never take this as an indication that the results are correct.

2.6 ACTIVITY-COEFFICIENT MODELS FOR THE LIQUID PHASE

In Sections 2.3 and 2.5, methods based on equations of state are presented for predicting thermodynamic properties of vapor and liquid mixtures. In this section, predictions of liquid properties based on *Gibbs free-energy models* for predicting liquid-phase activity coefficients and other excess functions such as volume and enthalpy of mixing are developed. Regular-solution theory, which can be applied to mixtures of nonpolar compounds using only constants for the pure components, is the first model presented. This is followed by a discussion of several models that can be applied to mixtures containing polar compounds, provided that experimental data are available to determine the *binary interaction parameters* in these models. If not, group-contribution methods, which have been extensively developed, can be used to make estimates. All models discussed can be applied to predict vapor–liquid phase equilibria; and some can estimate liquid–liquid equilibria, and even solid–liquid and polymer–liquid equilibria.

Except at high pressures, dependency of *K*-values on composition is due primarily to nonideal solution behavior in the liquid phase. Prausnitz, Edmister, and Chao [29] showed that the relatively simple *regular-solution theory* of Scatchard and Hildebrand [30] can be used to estimate deviations due to nonideal behavior of hydrocarbon–liquid mixtures. They expressed *K*-values in terms of (2-27), $K_i = \gamma_{iL}\phi_{iL}/\bar{\phi}_{iV}$. Chao and Seader [9] simplified and extended application of this equation to a general correlation for hydrocarbons and some light gases in the form of a compact set of equations

especially suitable for use with a digital computer, which was widely used before the availability of the S–R–K and P–R equations.

Simple models for the liquid-phase activity coefficient, γ_{iL}, based only on properties of pure species, are not generally accurate. However, for hydrocarbon mixtures, regular-solution theory is convenient and widely applied. The theory is based on the premise that nonideality is due to differences in van der Waals forces of attraction among the different molecules present. Regular solutions have an endothermic heat of mixing, and all activity coefficients are greater than one. These solutions are regular in the sense that molecules are assumed to be randomly dispersed. Unequal attractive forces between like and unlike molecule pairs tend to cause segregation of molecules. However, for regular solutions the species concentrations on a molecular level are identical to overall solution concentrations. Therefore, excess entropy due to segregation is zero and entropy of regular solutions is identical to that of ideal solutions, in which the molecules are randomly dispersed.

Activity Coefficients from Gibbs Free Energy

Activity-coefficient equations often have their basis in Gibbs free-energy models. For a nonideal solution, the molar Gibbs free energy, g, is the sum of the molar free energy of an ideal solution and an excess molar free energy g^E for nonideal effects. For a liquid solution,

$$\begin{aligned} g &= \sum_{i=1}^{C} x_i g_i + RT \sum_{i=1}^{C} x_i \ln x_i + g^E \\ &= \sum_{i=1}^{C} x_i \left(g_i + RT \ln x_i + \bar{g}_i^E\right) \end{aligned} \tag{2-58}$$

where $g \equiv h – Ts$ and excess molar free energy is the sum of the partial excess molar free energies. The partial excess molar free energy is related by classical thermodynamics to the liquid-phase activity coefficient by

$$\begin{aligned} \frac{\bar{g}_i^E}{RT} = \ln \gamma_i &= \left[\frac{\partial (N_t g^E/RT)}{\partial N_i}\right]_{P,T,N_j} \\ &= \frac{g^E}{RT} - \sum_k x_k \left[\frac{\partial (g^E/RT)}{\partial x_k}\right]_{P,T,x_r} \end{aligned} \tag{2-59}$$

where $j \neq i$, $r \neq k$, $k \neq i$, and $r \neq i$.

The relationship between excess molar free energy and excess molar enthalpy and entropy is

$$g^E = h^E - Ts^E = \sum_{i=1}^{C} x_i \left(\bar{h}_i^E - T\bar{s}_i^E\right) \tag{2-60}$$

Regular-Solution Model

For a multicomponent, regular liquid solution, the excess molar free energy is based on nonideality due to differences in molecular size and intermolecular forces. The former are expressed in terms of liquid molar volume and the latter in terms of the enthalpy of vaporization. The resulting model is

$$g^E = \sum_{i=1}^{C} (x_i v_{iL}) \left[\frac{1}{2} \sum_{i=1}^{C} \sum_{j=1}^{C} \Phi_i \Phi_j (\delta_i - \delta_j)^2\right] \tag{2-61}$$

where Φ is the volume fraction assuming additive molar volumes, as given by

$$\Phi_i = \frac{x_i v_{iL}}{\sum_{j=1}^{C} x_j v_{jL}} = \frac{x_i v_{iL}}{v_L} \tag{2-62}$$

and δ is the solubility parameter, which is defined in terms of the volumetric internal energy of vaporization as

$$\delta_i = \left(\frac{\Delta E_i^{\text{vap}}}{v_{iL}}\right)^{1/2} \tag{2-63}$$

Values of the solubility parameter for many components can be obtained from process simulation programs.

Applying (2-59) to (2-61) gives an expression for the activity coefficient in a regular solution:

$$\ln \gamma_{iL} = \frac{v_{iL} \left(\delta_i - \sum_{j=1}^{C} \Phi_j \delta_j\right)^2}{RT} \tag{2-64}$$

Because $\ln \gamma_{iL}$ varies almost inversely with absolute temperature, $v_i L$ and δ_j are frequently taken as constants at some convenient reference temperature, such as 25°C. Thus, the estimation of γ_L by regular-solution theory requires only the pure-species constants v_L and δ. The latter parameter is often treated as an empirical constant determined by back-calculation from experimental data. For species with a critical temperature below 25°C, v_L and δ at 25°C are hypothetical. However, they can be evaluated by back-calculation from phase-equilibria data.

When molecular-size differences, as reflected by liquid molar volumes, are appreciable, the following Flory–Huggins size correction can be added to the regular-solution free-energy contribution:

$$g^E = RT \sum_{i=1}^{C} x_i \ln \left(\frac{\Phi_i}{x_i}\right) \tag{2-65}$$

Substitution of (2-65) into (2-59) gives

$$\ln \gamma_{iL} = \ln \left(\frac{v_{iL}}{v_L}\right) + 1 - \left(\frac{v_{iL}}{v_L}\right) \tag{2-66}$$

The complete expression for the activity coefficient of a species in a regular solution, including the Flory–Huggins correction, is

$$\gamma_{iL} = \exp \left[\frac{v_{iL} \left(\delta_i - \sum_{j=1}^{C} \Phi_j \delta_j\right)^2}{RT} + \ln \left(\frac{v_{iL}}{v_L}\right) + 1 - \frac{v_{iL}}{v_L}\right] \tag{2-67}$$

EXAMPLE 2.7

Yerazunis, Plowright, and Smola [31] measured liquid-phase activity coefficients for the *n*-heptane/toluene system over the entire concentration range at 1 atm (101.3 kPa). Estimate activity coefficients for the range of conditions using regular-solution theory both with and without the Flory–Huggins correction. Compare estimated values with experimental data.

SOLUTION

Experimental liquid-phase compositions and temperatures for 7 of 19 points are as follows, where H denotes heptane and T denotes toluene:

T, °C	x_H	x_T
98.41	1.0000	0.0000
98.70	0.9154	0.0846
99.58	0.7479	0.2521
101.47	0.5096	0.4904
104.52	0.2681	0.7319
107.57	0.1087	0.8913
110.60	0.0000	1.0000

At 25°C, liquid molar volumes are $v_{H_L} = 147.5\ \text{cm}^3/\text{mol}$ and $v_{T_L} = 106.8\ \text{cm}^3/\text{mol}$. Solubility parameters are 7.43 and 8.914 $(\text{cal}/\text{cm}^3)^{1/2}$, respectively, for H and T. As an example, consider mole fractions in the above table for 104.52°C. From (2-62), volume fractions are

$$\Phi_H = \frac{0.2681(147.5)}{0.2681(147.5) + 0.7319(106.8)} = 0.3359$$

$$\Phi_T = 1 - \Phi_H = 1 - 0.3359 = 0.6641$$

Substitution of these values, together with the solubility parameters, into (2-64) gives

$$\gamma_H = \exp\left\{\frac{147.5[7.430 - 0.3359(7.430) - 0.6641(8.914)]^2}{1.987(377.67)}\right\} = 1.212$$

Values of γ_H and γ_T computed in this manner for all seven liquid-phase conditions are plotted in Figure 2.14.

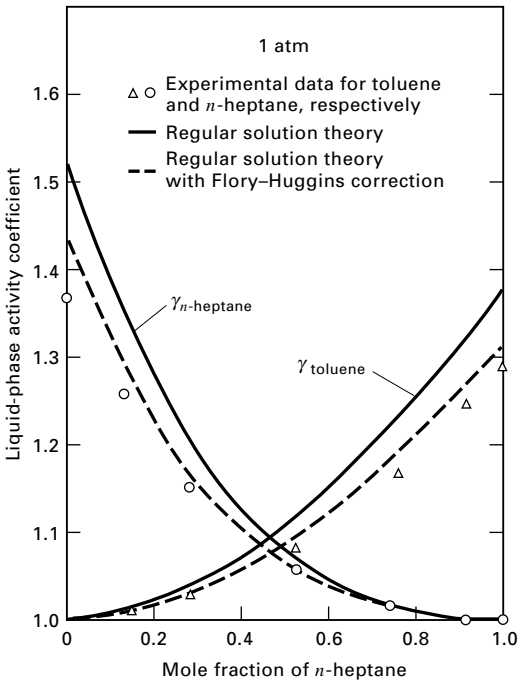

Figure 2.14 Liquid-phase activity coefficients for *n*-heptane/toluene system at 1 atm.

Applying (2-67), with the Flory–Huggins correction, to the same data point gives

$$\gamma_H = \exp\left[0.1923 + \ln\left(\frac{147.5}{117.73}\right) + 1 - \left(\frac{147.5}{117.73}\right)\right] = 1.179$$

Values of γ_H and γ_T computed in this manner are included in Figure 2.14. Deviations from experiment are not greater than 12% for regular-solution theory and not greater than 6% when the Flory–Huggins correction is included. Unfortunately, such good agreement is not always obtained with nonpolar hydrocarbon solutions, as shown, for example, by Hermsen and Prausnitz [32], who studied the cyclopentane/benzene system.

Nonideal Liquid Solutions

When liquids contain dissimilar polar species, particularly those that can form or break hydrogen bonds, the ideal-liquid solution assumption is almost always invalid and the regular-solution theory is not applicable. Ewell, Harrison, and Berg [33] provide a very useful classification of molecules based on the potential for association or solvation due to hydrogen-bond formation. If a molecule contains a hydrogen atom attached to a donor atom (O, N, F, and in certain cases C), the active hydrogen atom can form a bond with another molecule containing a donor atom. The classification in Table 2.7 permits qualitative estimates of deviations from Raoult's law for binary pairs when used in conjunction with Table 2.8. Positive deviations correspond to values of $\gamma_{iL} > 1$. Nonideality results in a variety of variations of γ_{iL} with composition, as shown in Figure 2.15 for several binary systems, where the Roman numerals refer to classification groups in Tables 2.7 and 2.8. Starting with Figure 2.15a and taking the other plots in order, we offer the following explanations for the nonidealities. Normal heptane (V) breaks ethanol (II) hydrogen bonds, causing strong positive deviations. In Figure 2.15b, similar but less positive deviations occur when acetone (III) is added to formamide (I). Hydrogen bonds are broken and formed with chloroform (IV) and methanol (II) in Figure 2.15c, resulting in an unusual positive deviation curve for chloroform that passes through a maximum. In Figure 2.15d, chloroform (IV) provides active hydrogen atoms that can form hydrogen bonds with oxygen atoms of acetone (III), thus causing negative deviations. For water (I) and *n*-butanol (II) in Figure 2.15e, hydrogen bonds of both molecules are broken, and nonideality is sufficiently strong to cause formation of two immiscible liquid phases (*phase splitting*) over a wide region of overall composition.

Table 2.7 Classification of Molecules Based on Potential for Forming Hydrogen Bonds

Class	Description	Example
I	Molecules capable of forming three-dimensional networks of strong H-bonds	Water, glycols, glycerol, amino alcohols, hydroxylamines, hydroxyacids, polyphenols, and amides
II	Other molecules containing both active hydrogen atoms and donor atoms (O, N, and F)	Alcohols, acids, phenols, primary and secondary amines, oximes, nitro and nitrile compounds with α-hydrogen atoms, ammonia, hydrazine, hydrogen fluoride, and hydrogen cyanide
III	Molecules containing donor atoms but no active hydrogen atoms	Ethers, ketones, aldehydes, esters, tertiary amines (including pyridine type), and nitro and nitrile compounds without α-hydrogen atoms
IV	Molecules containing active hydrogen atoms but no donor atoms that have two or three chlorine atoms on the same carbon atom as a hydrogen or one chlorine on the carbon atom and one or more chlorine atoms on adjacent carbon atoms	$CHCl_3$, CH_2Cl_2, CH_3CHCl_2, CH_2ClCH_2Cl, $CH_2ClCHClCH_2Cl$, and $CH_2ClCHCl_2$
V	All other molecules having neither active hydrogen atoms nor donor atoms	Hydrocarbons, carbon disulfide, sulfides, mercaptans, and halohydrocarbons not in class IV

Nonideal-solution effects can be incorporated into K-value formulations in two different ways. We have already described the use of $\bar{\phi}_i$, the partial fugacity coefficient, in conjunction with an equation of state and adequate mixing rules. This is the method most frequently used for handling nonidealities in the vapor phase. However, $\bar{\phi}_{iV}$ reflects the combined effects of a nonideal gas and a nonideal-gas solution. At low pressures, both effects are negligible. At moderate pressures, a vapor solution may still be ideal even though the gas mixture does not follow the ideal-gas law. Nonidealities in the liquid phase, however, can be severe even at low pressures. Earlier in this section, $\bar{\phi}_{iL}$ was used to express liquid-phase nonidealities for nonpolar species. When polar species are present, mixing rules can be modified to include binary interaction parameters, k_{ij}, as in (2-51).

The other technique for handling solution nonidealities is to retain $\bar{\phi}_{iV}$ in the K-value formulation, but replace $\bar{\phi}_{iL}$ by the product of γ_{iL} and ϕ_{iL}, where the former quantity accounts for deviations from nonideal solutions. Equation (2-26) then becomes

$$K_i = \frac{\gamma_{iL}\phi_{iL}}{\bar{\phi}_{iV}} \tag{2-68}$$

which was derived previously as (2-27). At low pressures, from Table 2.2, $\phi_{iL} = P_i^s/P$ and $\bar{\phi}_{iV} = 1.0$, so (2-68)

Table 2.8 Molecule Interactions Causing Deviations from Raoult's Law

Type of Deviation	Classes	Effect on Hydrogen Bonding
Always negative	III + IV	H-bonds formed only
Quasi-ideal; always positive or ideal	III + III III + V IV + IV IV + V V + V	No H-bonds involved
Usually positive, but some negative	I + I I + II I + III II + II II + III	H-bonds broken and formed
Always positive	I + IV (frequently limited solubility) II + IV	H-bonds broken and formed, but dissociation of Class I or II is more important effect
Always positive	I + V II + V	H-bonds broken only

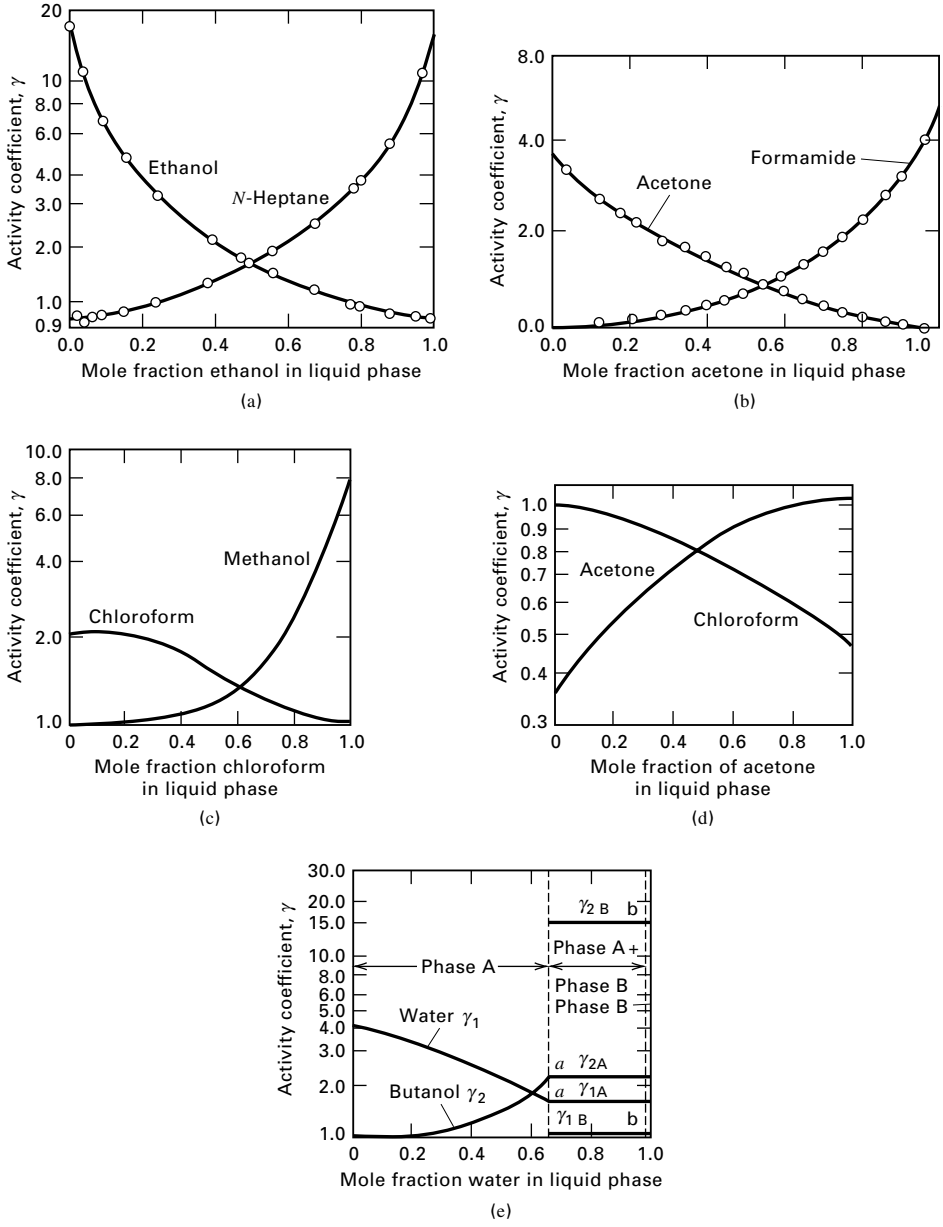

Figure 2.15 Typical variations of activity coefficients with composition in binary liquid systems: (a) ethanol(II)/*n*-heptane(V); (b) acetone(III)/formamide(I); (c) chloroform(IV)/methanol(II); (d) acetone(III)/chloroform(IV); (e) water(I)/*n*-butanol(II).

reduces to a modified Raoult's law K-value, which differs from (2-44) only in the γ_{iL} term:

$$K_i = \frac{\gamma_{iL} P_i^s}{P} \tag{2-69}$$

At moderate pressures, (5) of Table 2.3 is preferred over (2-69).

Regular-solution theory is useful only for estimating values of γ_{iL} for mixtures of nonpolar species. However, many empirical and semitheoretical equations exist for estimating activity coefficients of binary mixtures containing polar and/or nonpolar species. These equations contain binary interaction parameters, which are back-calculated from experimental data. Some of the more useful equations are listed in Table 2.9 in binary-pair form. For a given activity-coefficient correlation, the equations of Table 2.10 can be used to determine excess volume, excess enthalpy, and excess entropy. However, unless the dependency on pressure of the parameters and properties used in the equations for activity coefficient is known, excess liquid volumes cannot be determined directly from (1) of Table 2.10. Fortunately, the contribution of excess volume to total mixture volume is generally small for solutions of nonelectrolytes. For example, consider a 50 mol% solution of ethanol in *n*-heptane at 25°C. From Figure 2.15a, this is a highly nonideal, but miscible, liquid mixture. From the data of Van Ness, Soczek, and Kochar [34], excess volume is only 0.465 cm^3/mol, compared to an estimated ideal-solution molar volume of 106.3 cm^3/mol. Once the partial molar excess functions are estimated for each species, the excess functions are computed from the mole fraction sums.

Table 2.9 Empirical and Semitheoretical Equations for Correlating Liquid-Phase Activity Coefficients of Binary Pairs

Name	Equation for Species 1	Equation for Species 2
(1) Margules	$\log\ \gamma_1 = Ax_2^2$	$\log\ \gamma_2 = Ax_1^2$
(2) Margules (two-constant)	$\log\ \gamma_1 = x_2^2[\bar{A}_{12} + 2x_1(\bar{A}_{21} - \bar{A}_{12})]$	$\log\ \gamma_2 = x_1^2[\bar{A}_{21} + 2x_2(\bar{A}_{12} - \bar{A}_{21})]$
(3) van Laar (two-constant)	$\ln\gamma_1 = \dfrac{A_{12}}{[1 + (x_1A_{12})/(x_2A_{21})]^2}$	$\ln\gamma_2 = \dfrac{A_{21}}{[1 + (x_2A_{21})/(x_1A_{12})]^2}$
(4) Wilson (two-constant)	$\ln\gamma_1 = -\ln(x_1 + \Lambda_{12}x_2) + x_2\left(\dfrac{\Lambda_{12}}{x_1 + \Lambda_{12}x_2} - \dfrac{\Lambda_{21}}{x_2 + \Lambda_{21}x_1}\right)$	$\ln\gamma_2 = -\ln(x_2 + \Lambda_{21}x_1) - x_1\left(\dfrac{\Lambda_{12}}{x_1 + \Lambda_{12}x_2} - \dfrac{\Lambda_{21}}{x_2 + \Lambda_{21}x_1}\right)$
(5) NRTL (three-constant)	$\ln\gamma_1 = \dfrac{x_2^2\tau_{21}G_{21}^2}{(x_1 + x_2G_{21})^2} + \dfrac{x_1^2\tau_{12}G_{12}}{(x_2 + x_1G_{12})^2}$, $G_{ij} = \exp(-\alpha_{ij}\tau_{ij})$	$\ln\gamma_2 = \dfrac{x_1^2\tau_{12}G_{12}^2}{(x_2 + x_1G_{12})^2} + \dfrac{x_2^2\tau_{21}G_{21}}{(x_1 + x_2G_{21})^2}$, $G_{ij} = \exp(-\alpha_{ij}\tau_{ij})$
(6) UNIQUAC (two-constant)	$\ln\gamma_1 = \ln\dfrac{\Psi_1}{x_1} + \dfrac{\bar{Z}}{2}q_1\ln\dfrac{\theta_1}{\Psi_1} + \Psi_2\left(l_1 - \dfrac{r_1}{r_2}l_2\right) - q_1\ln(\theta_1 + \theta_2T_{21}) + \theta_2q_1\left(\dfrac{T_{21}}{\theta_1 + \theta_2T_{21}} - \dfrac{T_{12}}{\theta_2 + \theta_1T_{12}}\right)$	$\ln\gamma_2 = \ln\dfrac{\Psi_2}{x_2} + \dfrac{\bar{Z}}{2}q_2\ln\dfrac{\theta_2}{\Psi_2} + \Psi_1\left(l_2 - \dfrac{r_2}{r_1}l_1\right) - q_2\ln(\theta_2 + \theta_1T_{12}) + \theta_1q_2\left(\dfrac{T_{12}}{\theta_2 + \theta_1T_{12}} - \dfrac{T_{21}}{\theta_1 + \theta_2T_{21}}\right)$

Margules Equations

The Margules equations (1) and (2) in Table 2.9 date back to 1895, and the two-constant form is still in common use because of its simplicity. These equations result from power-series expansions in mole fractions for $\bar{g}_i^E$ and conversion to activity coefficients by means of (2-59). The one-constant form is equivalent to symmetrical activity-coefficient curves, which are rarely observed experimentally.

van Laar Equation

Because of its flexibility, simplicity, and ability to fit many systems well, the van Laar equation is widely used. It was derived from the van der Waals equation of state, but the constants, shown as A_{12} and A_{21} in (3) of Table 2.9, are best back-calculated from experimental data. These constants are, in theory, constant only for a particular binary pair at a given temperature. In practice, they are frequently computed from isobaric data covering a range of temperature. The van Laar theory expresses the temperature dependence of A_{ij} as

$$A_{ij} = \frac{A'_{ij}}{RT} \tag{2-70}$$

Regular-solution theory and the van Laar equation are equivalent for a binary solution if

$$A_{ij} = \frac{v_{iL}}{RT}(\delta_i - \delta_j)^2 \tag{2-71}$$

The van Laar equation can fit activity coefficient–composition curves corresponding to both positive and negative deviations from Raoult's law, but cannot fit curves that exhibit minima or maxima such as those in Figure 2.15c.

When data are isothermal, or isobaric over only a narrow range of temperature, determination of van Laar constants is conducted in a straightforward manner. The most accurate procedure is a nonlinear regression to obtain the best fit to the data over the entire range of binary composition, subject to minimization of some objective function. A less accurate, but extremely rapid, manual-calculation procedure can be used when experimental data can be extrapolated to infinite-dilution conditions. Modern experimental techniques are available for accurately and rapidly determining activity

Table 2.10 Classical Partial Molar Excess Functions of Thermodynamics

Excess volume:

(1) $\left(\bar{v}_{iL} - \bar{v}_{iL}^{\mathrm{ID}}\right) \equiv \bar{v}_{iL}^{\mathrm{E}} = RT\left(\dfrac{\partial \ln\gamma_{iL}}{\partial P}\right)_{T,x}$

Excess enthalpy:

(2) $\left(\bar{h}_{iL} - \bar{h}_{iL}^{\mathrm{ID}}\right) \equiv \bar{h}_{iL}^{\mathrm{E}} = -RT^2\left(\dfrac{\partial \ln\gamma_{iL}}{\partial T}\right)_{P,x}$

Excess entropy:

(3) $\left(\bar{s}_{iL} - \bar{s}_{iL}^{\mathrm{ID}}\right) \equiv \bar{s}_{iL}^{\mathrm{E}} = -R\left[T\left(\dfrac{\partial \ln\gamma_{iL}}{\partial T}\right)_{P,x} + \ln\gamma_{iL}\right]$

ID = ideal mixture; E = excess because of nonideality.

coefficients at infinite dilution. Applying (3) of Table 2.9 to the conditions $x_i = 0$ and then $x_j = 0$, we have

$$A_{ij} = \ln \gamma_i^{\infty}, \quad x_i = 0$$

and

$$A_{ji} = \ln \gamma_j^{\infty}, \quad x_j = 0 \tag{2-72}$$

For practical applications, it is important that the van Laar equation predicts azeotrope formation correctly, where $x_i = y_i$ and $K_i = 1.0$. If activity coefficients are known or can be computed at the azeotropic composition—say, from (2-69), ($\gamma_{iL} = P/P_i^s$, since $K_i = 1.0$)—these coefficients can be used to determine the van Laar constants directly from the following equations obtained by solving simultaneously for A_{12} and A_{21}:

$$A_{12} = \ln \gamma_1 \left(1 + \frac{x_2 \ln \gamma_2}{x_1 \ln \gamma_1}\right)^2 \tag{2-73}$$

$$A_{21} = \ln \gamma_2 \left(1 + \frac{x_1 \ln \gamma_1}{x_2 \ln \gamma_2}\right)^2 \tag{2-74}$$

These equations are applicable to activity-coefficient data obtained at any single composition.

Mixtures of self-associated polar molecules (class II in Table 2.7) with nonpolar molecules such as hydrocarbons (class V) can exhibit the strong nonideality of the positive-deviation type shown in Figure 2.15a. Figure 2.16 shows experimental data of Sinor and Weber [35] for ethanol (1)/*n*-hexane (2), a system of this type, at 101.3 kPa. These data were correlated with the van Laar equation by Orye and Prausnitz [36] to give $A_{12} = 2.409$ and $A_{21} = 1.970$. From $x_1 = 0.1$ to 0.9, the fit of the data to the van Laar equation is reasonably good; in the dilute regions, however, deviations are quite severe and the predicted activity coefficients for ethanol are low. An even more serious problem with these highly nonideal mixtures is that the van Laar equation may erroneously predict formation of two liquid phases (phase splitting) when values of activity coefficients exceed approximately 7.

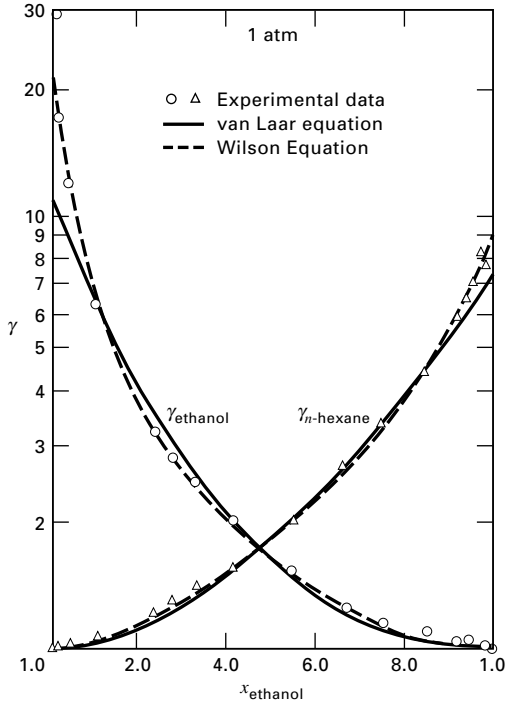

Figure 2.16 Liquid-phase activity coefficients for ethanol/*n*-hexane system.

[Data from J.E. Sinor and J.H. Weber, *J. Chem. Eng. Data,* **5,** 243–247 (1960).]

Local-Composition Concept and the Wilson Model

Since its introduction in 1964, the Wilson equation [37], shown in binary form in Table 2.9 as (4), has received wide attention because of its ability to fit strongly nonideal, but miscible, systems. As shown in Figure 2.16, the Wilson equation, with binary interaction parameters of $\Lambda_{12} = 0.0952$ and $\Lambda_{21} = 0.2713$ determined by Orye and Prausnitz [36], fits experimental data well even in dilute regions where the variation of γ_1 becomes exponential. Corresponding infinite-dilution activity coefficients computed from the Wilson equation are $\gamma_1^{\infty} = 21.72$ and $\gamma_2^{\infty} = 9.104$.

The Wilson equation accounts for effects of differences both in molecular size and intermolecular forces, consistent with a semitheoretical interpretation based on the Flory–Huggins relation (2-65). Overall solution-volume fractions ($\Phi_i = x_i v_{iL}/v_L$) are replaced by local-volume fractions, $\bar{\Phi}_i$, which are related to local-molecule segregations caused by differing energies of interaction between pairs of molecules. The concept of local compositions that differ from overall compositions is shown schematically for an overall, equimolar, binary solution in Figure 2.17, which is taken from Cukor and Prausnitz [38]. About a central molecule of type 1, the local mole fraction of molecules of type 2 is shown as $\frac{5}{8}$, while the overall composition is $\frac{1}{2}$.

For local-volume fraction, Wilson proposed

$$\bar{\Phi}_i = \frac{v_{iL} x_i \exp(-\lambda_{ii}/RT)}{\sum_{j=1}^{C} v_{jL} x_j \exp(-\lambda_{ij}/RT)} \tag{2-75}$$

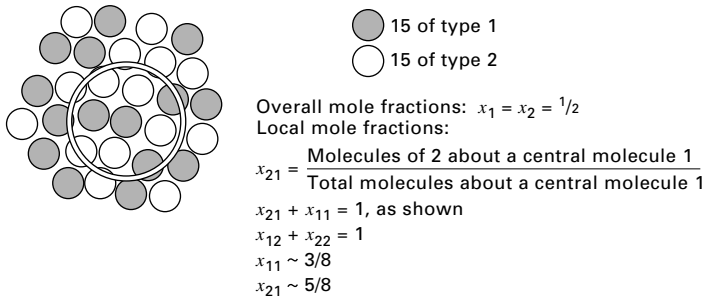

Figure 2.17 The concept of local compositions.

[From P.M. Cukor and J.M. Prausnitz, *Int. Chem. Eng. Symp. Ser. No.* 32, **3,** 88 (1969).]

where energies of interaction $\lambda_{ij} = \lambda_{ji}$, but $\lambda_{ii} \neq \lambda_{jj}$. Following the treatment by Orye and Prausnitz [36], substitution of the binary form of (2-75) into (2-65) and defining the binary interaction parameters as

$$\Lambda_{12} = \frac{v_{2L}}{v_{1L}} \exp\left[-\frac{(\lambda_{12} - \lambda_{11})}{RT}\right] \tag{2-76}$$

$$\Lambda_{21} = \frac{v_{1L}}{v_{2L}} \exp\left[-\frac{(\lambda_{12} - \lambda_{22})}{RT}\right] \tag{2-77}$$

leads to the following equation for a binary system:

$$\frac{g^E}{RT} = -x_1 \ln(x_1 + \Lambda_{12}x_2) - x_2 \ln(x_2 + \Lambda_{21}x_1) \tag{2-78}$$

The Wilson equation is very effective for dilute compositions where entropy effects dominate over enthalpy effects. The Orye–Prausnitz form of the Wilson equation for the activity coefficient, as given in Table 2.9, follows from combining (2-59) with (2-78). Values of $\Lambda_{ij} < 1$ correspond to positive deviations from Raoult's law, while values > 1 correspond to negative deviations. Ideal solutions result from $\Lambda_{ij} = 1$. Studies indicate that λ_{ii} and λ_{ij} are temperature-dependent. Values of v_{iL}/v_{jL} depend on temperature also, but the variation may be small compared to temperature effects on the exponential terms in (2-76) and (2-77).

The Wilson equation is readily extended to multicomponent mixtures by neglecting ternary and higher molecular interactions and assuming a pseudo-binary mixture. The following multicomponent Wilson equation involves only binary interaction constants:

$$\ln \gamma_k = 1 - \ln\left(\sum_{j=1}^{C} x_j \Lambda_{kj}\right) - \sum_{i=1}^{C}\left(\frac{x_i \Lambda_{ik}}{\sum_{j=1}^{C} x_j \Lambda_{ij}}\right) \tag{2-79}$$

where $\Lambda_{ii} = \Lambda_{jj} = \Lambda_{kk} = 1$.

As mixtures become highly nonideal, but still miscible, the Wilson equation becomes markedly superior to the Margules and van Laar equations. The Wilson equation is consistently superior for multicomponent solutions. Values of the constants in the Wilson equation for many binary systems are tabulated in the DECHEMA collection of Gmehling and Onken [39]. Two limitations of the Wilson equation are its inability to predict immiscibility, as in Figure 2.15e, and maxima and minima in the activity coefficient–mole fraction relationships, as shown in Figure 2.15c.

When insufficient experimental data are available to determine binary Wilson parameters from a best fit of activity coefficients over the entire range of composition, infinite-dilution or single-point values can be used. At infinite dilution, the Wilson equation in Table 2.9 becomes

$$\ln \gamma_1^{\infty} = 1 - \ln \Lambda_{12} - \Lambda_{21} \tag{2-80}$$

$$\ln \gamma_2^{\infty} = 1 - \ln \Lambda_{21} - \Lambda_{12} \tag{2-81}$$

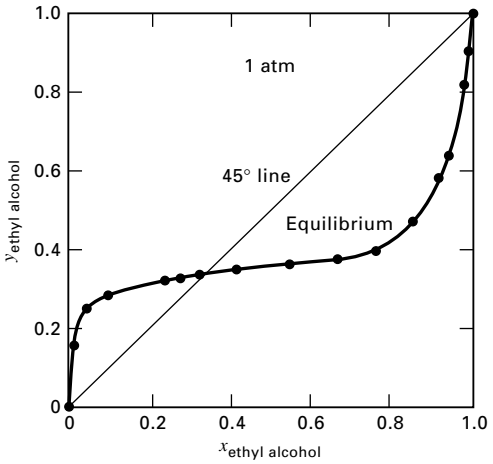

Figure 2.18 Equilibrium curve for *n*-hexane/ethanol system.

An iterative procedure is required to obtain Λ_{12} and Λ_{21} from these nonlinear equations. If temperatures corresponding to γ_1^{∞} and γ_2^{∞} are not close or equal, (2-76) and (2-77) should be substituted into (2-80) and (2-81) with values of $(\lambda_{12} - \lambda_{11})$ and $(\lambda_{12} - \lambda_{22})$ determined from estimates of pure-component liquid molar volumes.

When the experimental data of Sinor and Weber [35] for *n*-hexane/ethanol, shown in Figure 2.16, are plotted as a *y*–*x* diagram in ethanol (Figure 2.18), the equilibrium curve crosses the 45° line at an ethanol mole fraction of $x = 0.332$. The measured temperature corresponding to this composition is 58°C. Ethanol has a normal boiling point of 78.33°C, which is higher than the normal boiling point of 68.75°C for *n*-hexane. Nevertheless, ethanol is more volatile than *n*-hexane up to an ethanol mole fraction of $x = 0.322$, the minimum-boiling azeotrope. This occurs because of the relatively close boiling points of the two species and the high activity coefficients for ethanol at low concentrations. At the azeotropic composition, $y_i = x_i$; therefore, $K_i = 1.0$. Applying (2-69) to both species,

$$\gamma_1 P_1^s = \gamma_2 P_2^s \tag{2-82}$$

If species 2 is more volatile in the pure state ($P_2^s > P_1^s$), the criteria for formation of a minimum-boiling azeotrope are

$$\gamma_1 \geq 1 \tag{2-83}$$

$$\gamma_2 \geq 1 \tag{2-84}$$

and

$$\frac{\gamma_1}{\gamma_2} < \frac{P_2^s}{P_1^s} \tag{2-85}$$

for x_1 less than the azeotropic composition. These critieria are most readily applied at $x_1 = 0$. For example, for the *n*-hexane (2)/ethanol (1) system at 1 atm (101.3 kPa), when the liquid-phase mole fraction of ethanol approaches zero, temperature approaches 68.75°C (155.75°F), the boiling point of pure *n*-hexane. At this temperature, $P_1^s = 10$ psia

(68.9 kPa) and $P_2^s = 14.7$ psia (101.3 kPa). Also from Figure 2.16, $\gamma_1^\infty = 21.72$ when $\gamma_2 = 1.0$. Thus, $\gamma_1^\infty/\gamma_2 = 21.72$, but $P_2^s/P_1^s = 1.47$. Therefore, a minimum-boiling azeotrope will occur.

Maximum-boiling azeotropes are less common. They occur for relatively close-boiling mixtures when negative deviations from Raoult's law arise such that $\gamma_i < 1.0$. Criteria for their formation are derived in a manner similar to that for minimum-boiling azeotropes. At $x_1 = 1$, where species 2 is more volatile,

$$\gamma_1 = 1.0 \tag{2-86}$$

$$\gamma_2^\infty < 1.0 \tag{2-87}$$

and

$$\frac{\gamma_2^\infty}{\gamma_1} < \frac{P_1^s}{P_2^s} \tag{2-88}$$

For an azeotropic binary system, the two binary interaction parameters Λ_{12} and Λ_{21} can be determined by solving (4) of Table 2.9 at the azeotropic composition, as shown in the following example.

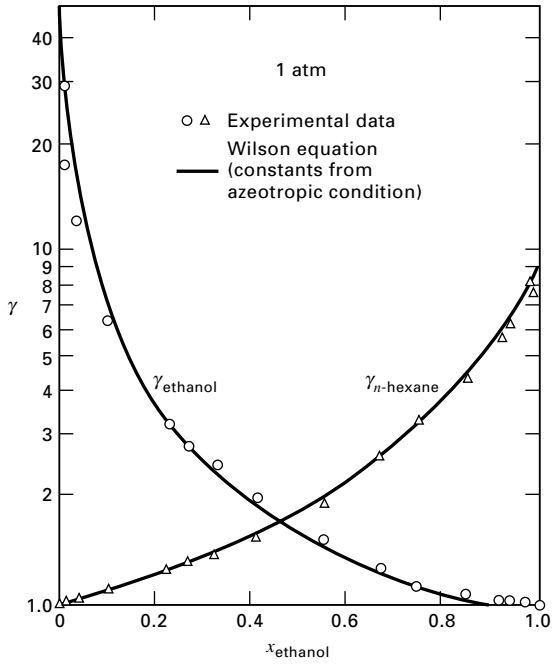

Figure 2.19 Liquid-phase activity coefficients for ethanol/*n*-hexane system.

EXAMPLE 2.8

From measurements by Sinor and Weber [35] of the azeotropic condition for the ethanol/*n*-hexane system at 1 atm (101.3 kPa, 14.696 psia), calculate Λ_{12} and Λ_{21}.

SOLUTION

Let E denote ethanol and H denote *n*-hexane. The azeotrope occurs at $x_E = 0.332$, $x_H = 0.668$, and $T = 58°C$ (331.15 K). At 1 atm, (2-69) can be used to approximate *K*-values. Thus, at azeotropic conditions, $\gamma_i = P/P_i^s$. The vapor pressures at 58°C are $P_E^s = 6.26$ psia and $P_H^s = 10.28$ psia. Therefore,

$$\gamma_E = \frac{14.696}{6.26} = 2.348$$

$$\gamma_H = \frac{14.696}{10.28} = 1.430$$

Substituting these values together with the above corresponding values of x_i into the binary form of the Wilson equation in Table 2.9 gives

$$\ln 2.348 = -\ln(0.332 + 0.668\Lambda_{EH}) + 0.668\left(\frac{\Lambda_{EH}}{0.332 + 0.668\Lambda_{EH}} - \frac{\Lambda_{HE}}{0.332\Lambda_{HE} + 0.668}\right)$$

$$\ln 1.430 = -\ln(0.668 + 0.332\Lambda_{HE}) - 0.332\left(\frac{\Lambda_{EH}}{0.332 + 0.668\Lambda_{EH}} - \frac{\Lambda_{HE}}{0.332\Lambda_{HE} + 0.668}\right)$$

Solving these two nonlinear equations simultaneously by an iterative procedure, we obtain $\Lambda_{EH} = 0.041$ and $\Lambda_{HE} = 0.281$. From these constants, the activity-coefficient curves can be predicted if the temperature variations of Λ_{EH} and Λ_{HE} are ignored. The results are plotted in Figure 2.19. The fit of experimental data is good except, perhaps, for near-infinite-dilution conditions, where $\gamma_E^\infty = 49.82$ and $\gamma_H^\infty = 9.28$. The former value is considerably greater than the value of 21.72 obtained by Orye and Prausnitz [36] from a fit of all experimental data points. However, if Figures 2.16 and 2.19 are compared, it is seen that widely differing γ_E^∞ values have little effect on γ in the composition region $x_E = 0.15$ to 1.00, where the two sets of Wilson curves are almost identical. For accuracy over the entire composition range, commensurate with the ability of the Wilson equation, data for at least three well-spaced liquid compositions per binary are preferred.

The Wilson equation can be extended to liquid–liquid or vapor–liquid–liquid systems by multiplying the right-hand side of (2-78) by a third binary-pair constant evaluated from experimental data [37]. However, for multicomponent systems of three or more species, the third binary-pair constants must be the same for all constituent binary pairs. Furthermore, as shown by Hiranuma [40], representation of ternary systems involving only one partially miscible binary pair can be extremely sensitive to the third binary-pair Wilson constant. For these reasons, application of the Wilson equation to liquid–liquid systems has not been widespread. Rather, the success of the Wilson equation for prediction of activity coefficients for miscible liquid systems greatly stimulated further development of the local-composition concept of Wilson in an effort to obtain more universal expressions for liquid-phase activity coefficients.

NRTL Model

The nonrandom, two-liquid (NRTL) equation developed by Renon and Prausnitz [41,42] as listed in Table 2.9, represents an accepted extension of Wilson's concept. The NRTL equation is applicable to multicomponent vapor–liquid,

liquid–liquid, and vapor–liquid–liquid systems. For multicomponent vapor–liquid systems, only binary-pair constants from the corresponding binary-pair experimental data are required. For a multicomponent system, the NRTL expression for the activity coefficient is

$$\ln \gamma_i = \frac{\sum_{j=1}^{C} \tau_{ji} G_{ji} x_j}{\sum_{k=1}^{C} G_{ki} x_k} + \sum_{j=1}^{C} \left[\frac{x_j G_{ij}}{\sum_{k=1}^{C} G_{kj} x_k} \left(\tau_{ij} - \frac{\sum_{k=1}^{C} x_k \tau_{kj} G_{kj}}{\sum_{k=1}^{C} G_{kj} x_k} \right) \right] \tag{2-89}$$

where

$$G_{ji} = \exp(-\alpha_{ji} \tau_{ji}) \tag{2-90}$$

The coefficients τ are given by

$$\tau_{ij} = \frac{g_{ij} - g_{jj}}{RT} \tag{2-91}$$

$$\tau_{ji} = \frac{g_{ji} - g_{ii}}{RT} \tag{2-92}$$

where g_{ij}, g_{jj}, and so on are energies of interaction between molecule pairs. In the above equations, $G_{ji} \neq G_{ij}, \tau_{ij} \neq \tau_{ji}$, $G_{ii} = G_{jj} = 1$, and $\tau_{ii} = \tau_{jj} = 0$. Often $(g_{ij} - g_{jj})$ and other constants are linear in temperature. For ideal solutions, $\tau_{ji} = 0$.

The parameter α_{ji} characterizes the tendency of species j and species i to be distributed in a nonrandom fashion. When $\alpha_{ji} = 0$, local mole fractions are equal to overall solution mole fractions. Generally α_{ji} is independent of temperature and depends on molecule properties in a manner similar to the classifications in Tables 2.7 and 2.8. Values of α_{ji} usually lie between 0.2 and 0.47. When $\alpha_{ji} < 0.426$, phase immiscibility is predicted. Although α_{ji} can be treated as an adjustable parameter, to be determined from experimental binary-pair data, more commonly α_{ji} is set according to the following rules, which are occasionally ambiguous:

1. $\alpha_{ji} = 0.20$ for mixtures of saturated hydrocarbons and polar, nonassociated species (e.g., *n*-heptane/acetone).
2. $\alpha_{ji} = 0.30$ for mixtures of nonpolar compounds (e.g., benzene/*n*-heptane), except fluorocarbons and paraffins; mixtures of nonpolar and polar, nonassociated species (e.g., benzene/acetone); mixtures of polar species that exhibit negative deviations from Raoult's law (e.g., acetone/chloroform) and moderate positive deviations (e.g., ethanol/water); mixtures of water and polar nonassociated species (e.g., water/acetone).
3. $\alpha_{ji} = 0.40$ for mixtures of saturated hydrocarbons and homolog perfluorocarbons (e.g., *n*-hexane/perfluoro-*n*-hexane).
4. $\alpha_{ji} = 0.47$ for mixtures of an alcohol or other strongly self-associated species with nonpolar species (e.g., ethanol/benzene); mixtures of carbon tetrachloride with either acetonitrile or nitromethane; mixtures of water with either butyl glycol or pyridine.

UNIQUAC Model

In an attempt to place calculations of liquid-phase activity coefficients on a simple, yet more theoretical basis, Abrams and Prausnitz [43] used statistical mechanics to derive an expression for excess free energy. Their model, called UNIQUAC (universal quasichemical), generalizes a previous analysis by Guggenheim and extends it to mixtures of molecules that differ appreciably in size and shape. As in the Wilson and NRTL equations, local concentrations are used. However, rather than local volume fractions or local mole fractions, UNIQUAC uses the local area fraction θ_{ij} as the primary concentration variable.

The local area fraction is determined by representing a molecule by a set of bonded segments. Each molecule is characterized by two structural parameters that are determined relative to a standard segment taken as an equivalent sphere of a unit of a linear, infinite-length, polymethylene molecule. The two structural parameters are the relative number of segments per molecule, r (volume parameter), and the relative surface area of the molecule, q (surface parameter). Values of these parameters computed from bond angles and bond distances are given by Abrams and Prausnitz [43] and Gmehling and Onken [39] for a number of species. For other compounds, values can be estimated by the group-contribution method of Fredenslund et al. [46].

For a multicomponent liquid mixture, the UNIQUAC model gives the excess free energy as

$$\frac{g^E}{RT} = \sum_{i=1}^{C} x_i \ln \left(\frac{\Psi_i}{x_i} \right) + \frac{\bar{Z}}{2} \sum_{i=1}^{C} q_i x_i \ln \left(\frac{\theta_i}{\Psi_i} \right) - \sum_{i=1}^{C} q_i x_i \ln \left(\sum_{j=1}^{C} \theta_i T_{ji} \right) \tag{2-93}$$

The first two terms on the right-hand side account for *combinatorial* effects due to differences in molecule size and shape; the last term provides a *residual* contribution due to differences in intermolecular forces, where

$$\Psi_i = \frac{x_i r_i}{\sum_{i=1}^{C} x_i r_i} = \text{segment fraction} \tag{2-94}$$

$$\theta = \frac{x_i q_i}{\sum_{i=1}^{C} x_i q_i} = \text{area fraction} \tag{2-95}$$

where $\bar{Z}$ = lattice coordination number set equal to 10, and

$$T_{ji} = \exp \left(\frac{u_{ji} - u_{ii}}{RT} \right) \tag{2-96}$$

Equation (2-93) contains only two adjustable parameters for each binary pair, $(u_{ji} - u_{ii})$ and $(u_{ij} - u_{jj})$. Abrams and Prausnitz show that $u_{ji} = u_{ij}$ and $T_{ii} = T_{jj} = 1$. In general, $(u_{ji} - u_{ii})$ and $(u_{ij} - u_{jj})$ are linear functions of temperature.

If (2-59) is combined with (2-93), an equation for the liquid-phase activity coefficient for a species in a multicomponent mixture is obtained:

$$\ln \gamma_i = \ln \gamma_i^C + \ln \gamma_i^R$$

$$= \underbrace{\ln(\Psi_i/x_i) + (\bar{Z}/2)\, q_i \ln(\theta_i/\Psi_i) + l_i - (\Psi_i/x_i)\sum_{j=1}^{C} x_j l_j}_{C,\ \text{combinatorial}}$$

$$+ \underbrace{q_i \left[1 - \ln\left(\sum_{j=1}^{C} \theta_j T_{ji}\right) - \sum_{j=1}^{C} \left(\frac{\theta_j T_{ij}}{\sum_{k=1}^{C} \theta_k T_{kj}} \right) \right]}_{R,\ \text{residual}} \tag{2-97}$$

where

$$l_j = \left(\frac{\bar{Z}}{2}\right)(r_j - q_j) - (r_j - 1) \tag{2-98}$$

For a binary mixture of species 1 and 2, (2-97) reduces to (6) in Table 2.9 for $\bar{Z} = 10$.

UNIFAC Model

Liquid-phase activity coefficients must be estimated for nonideal mixtures even when experimental phase equilibria data are not available and when the assumption of regular solutions is not valid because polar compounds are present. For such predictions, Wilson and Deal [47] and then Derr and Deal [48], in the 1960s, presented methods based on treating a solution as a mixture of functional groups instead of molecules. For example, in a solution of toluene and acetone, the contributions might be 5 aromatic CH groups, 1 aromatic C group, and 1 CH_3 group from toluene; and 2 CH_3 groups plus 1 CO carbonyl group from acetone. Alternatively, larger groups might be employed to give 5 aromatic CH groups and 1 CCH_3 group from toluene; and 1 CH_3 group and 1 CH_3CO group from acetone. As larger and larger functional groups are used, the accuracy of molecular representation increases, but the advantage of the group-contribution method decreases because a larger number of groups is required. In practice, about 50 functional groups are used to represent literally thousands of multicomponent liquid mixtures.

To estimate the partial molar excess free energies, $\bar{g}_i^E$, and then the activity coefficients, size parameters for each functional group and binary interaction parameters for each pair of functional groups are required. Size parameters can be calculated from theory. Interaction parameters are back-calculated from existing phase-equilibria data and then used with the size parameters to predict phase-equilibria properties of mixtures for which no data are available.

The UNIFAC (UNIQUAC Functional-group Activity Coefficients) group-contribution method, first presented by Fredenslund, Jones, and Prausnitz [49] and further developed for use in practice by Fredenslund, Gmehling, and Rasmussen [50], Gmehling, Rasmussen, and Fredenslund [51], and Larsen, Rasmussen, and Fredenslund [52], has several advantages over other group-contribution methods: (1) It is theoretically based on the UNIQUAC method; (2) the parameters are essentially independent of temperature; (3) size and binary interaction parameters are available for a wide range of types of functional groups; (4) predictions can be made over a temperature range of 275–425 K and for pressures up to a few atmospheres; and (5) extensive comparisons with experimental data are available. All components in the mixture must be condensable.

The UNIFAC method for predicting liquid-phase activity coefficients is based on the UNIQUAC equation (2-97), wherein the molecular volume and area parameters in the combinatorial terms are replaced by

$$r_i = \sum_k \nu_k^{(i)} R_k \tag{2-99}$$

$$q_i = \sum_k \nu_k^{(i)} Q_k \tag{2-100}$$

where $\nu_k^{(i)}$ is the number of functional groups of type k in molecule i, and R_k and Q_k are the volume and area parameters, respectively, for the type-k functional group.

The residual term in (2-97), which is represented by $\ln \gamma_i^R$, is replaced by the expression

$$\ln \gamma_i^R = \underbrace{\sum_k \nu_k^{(i)} \left(\ln \Gamma_k - \ln \Gamma_k^{(i)} \right)}_{\text{all functional groups in mixture}} \tag{2-101}$$

where Γ_k is the residual activity coefficient of the functional group k in the actual mixture, and $\Gamma_k^{(i)}$ is the same quantity but in a reference mixture that contains only molecules of type i. The latter quantity is required so that $\gamma_i^R \to 1.0$ as $x_i \to 1.0$. Both Γ_k and $\Gamma_k^{(i)}$ have the same form as the residual term in (2-97). Thus,

$$\ln \Gamma_k = Q_k \left[1 - \ln\left(\sum_m \theta_m T_{mk}\right) - \sum_m \frac{\theta_m T_{mk}}{\sum_n \theta_n T_{nm}} \right] \tag{2-102}$$

where θ_m is the area fraction of group m, given by an equation similar to (2-95),

$$\theta_m = \frac{X_m Q_m}{\sum_n X_n Q_m} \tag{2-103}$$

where X_m is the mole fraction of group m in the solution,

$$X_m = \frac{\sum_j \nu_m^{(j)} x_j}{\sum_j \sum_n (\nu_n^{(j)} x_j)} \tag{2-104}$$

and T_{mk} is a group interaction parameter given by an equation similar to (2-96),

$$T_{mk} = \exp\left(-\frac{a_{mk}}{T}\right) \tag{2-105}$$

where $a_{mk} \neq a_{km}$. When $m = k$, then $a_{mk} = 0$ and $T_{mk} = 1.0$. For $\Gamma_k^{(i)}$, (2-102) also applies, where θ terms correspond to the pure component i. Although values of R_k and Q_k are different for each functional group, values of a_{mk} are equal for all subgroups within a main group. For example, main group CH_2 consists of subgroups CH_3, CH_2, CH, and C. Accordingly,

$$a_{CH_3,CHO} = a_{CH_2,CHO} = a_{CH,CHO} = a_{C,CHO}$$

Thus, the amount of experimental data required to obtain values of a_{mk} and a_{km} and the size of the corresponding bank of data for these parameters is not as large as might be expected.

The ability of a group-contribution method to predict liquid-phase activity coefficients has been further improved by introduction of a modified UNIFAC method by Gmehling [51], referred to as UNIFAC (Dortmund). To correlate data for mixtures having a wide range of molecular size, they modified the combinatorial part of (2-97). To handle temperature dependence more accurately, they replaced (2-105) with a three-coefficient equation. The resulting modification permits reasonably reliable predictions of liquid-phase activity coefficients (including applications to dilute solutions and multiple liquid phases), heats of mixing, and azeotropic compositions. Values of the UNIFAC (Dortmund) parameters for 51 groups are available in a series of publications starting in 1993 with Gmehling, Li, and Schiller [53] and more recently with Wittig, Lohmann, and Gmehling [54].

Liquid–Liquid Equilibria

When species are notably dissimilar and activity coefficients are large, two and even more liquid phases may coexist at equilibrium. For example, consider the binary system of methanol (1) and cyclohexane (2) at 25°C. From measurements of Takeuchi, Nitta, and Katayama [55], van Laar constants are $A_{12} = 2.61$ and $A_{21} = 2.34$, corresponding, respectively, to infinite-dilution activity coefficients of 13.6 and 10.4 obtained using (2-72). These values of A_{12} and A_{21} can be used to construct an equilibrium plot of y_1 against x_1 assuming an isothermal condition. By combining (2-69), where $K_i = y_i/x_i$, with

$$P = \sum_{i=1}^{C} x_i \gamma_{iL} P_i^s \tag{2-106}$$

one obtains the following relation for computing y_i from x_i:

$$y_1 = \frac{x_1 \gamma_1 P_1^s}{x_1 \gamma_1 P_1^s + x_2 \gamma_2 P_2^s} \tag{2-107}$$

Vapor pressures at 25°C are $P_1^s = 2.452$ psia (16.9 kPa) and $P_2^s = 1.886$ psia (13.0 kPa). Activity coefficients can be computed from the van Laar equation in Table 2.9. The resulting equilibrium plot is shown in Figure 2.20, where it is observed that over much of the liquid-phase region, three values of y_1 exist. This indicates phase instability. Experimentally, single liquid phases can exist only for cyclohexane-rich mixtures of

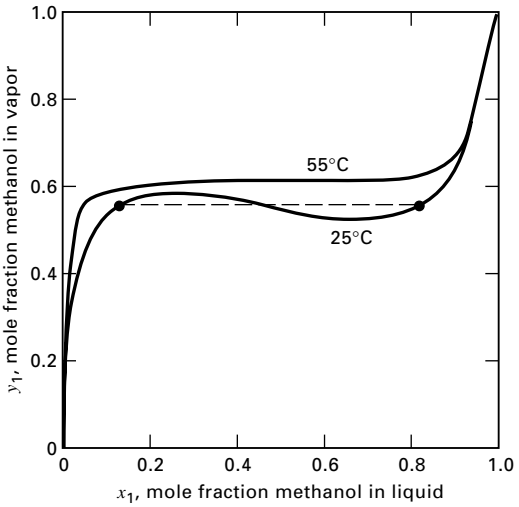

Figure 2.20 Equilibrium curves for methanol/cyclohexane systems.

[Data from K. Strubl, V. Svoboda, R. Holub, and J. Pick, *Collect. Czech. Chem. Commun.*, **35,** 3004–3019 (1970).]

$x_1 = 0.8248$ to 1.0 and for methanol-rich mixtures of $x_1 = 0.0$ to 0.1291. Because a coexisting vapor phase exhibits only a single composition, two coexisting liquid phases prevail at opposite ends of the dashed line in Figure 2.20. The liquid phases represent solubility limits of methanol in cyclohexane and cyclohexane in methanol.

For two coexisting equilibrium liquid phases, the relation $\gamma_{iL}^{(1)} x_i^{(1)} = \gamma_{iL}^{(2)} x_i^{(2)}$ must hold. This permits determination of the two-phase region in Figure 2.20 from the van Laar or other suitable activity-coefficient equation for which the constants are known. Also shown in Figure 2.20 is an equilibrium curve for the same binary system at 55°C based on data of Strubl et al. [56]. At this higher temperature, methanol and cyclohexane are completely miscible. The data of Kiser, Johnson, and Shetlar [57] show that phase instability ceases to exist at 45.75°C, the critical solution temperature. Rigorous thermodynamic methods for determining phase instability and, thus, existence of two equilibrium liquid phases are generally based on free-energy calculations, as discussed by Prausnitz et al. [4]. Most of the empirical and semitheoretical equations for the liquid-phase activity coefficient listed in Table 2.9 apply to liquid–liquid systems. The Wilson equation is a notable exception.

2.7 DIFFICULT MIXTURES

The equation-of-state and activity-coefficient models presented in Sections 2.5 and 2.6, respectively, are inadequate for estimating K-values of mixtures containing: (1) both polar and supercritical (light-gas) components, (2) electrolytes, and (3) both polymers and solvents. For these difficult mixtures, special models have been developed, some of which are briefly described in the following subsections. More detailed discussions of the following three topics are given by Prausnitz, Lichtenthaler, and de Azevedo [4].

Predictive Soave–Redlich–Kwong (PSRK) Model

Equation-of-state models, such as S–R–K and P–R, describe mixtures of nonpolar and slightly polar compounds. Gibbs free-energy activity-coefficient models are formulated for subcritical nonpolar and polar compounds. When a mixture contains both polar compounds and supercritical (light-gas) components (e.g., a mixture of hydrogen, carbon monoxide, methane, methyl acetate, and ethanol), neither method applies. To estimate vapor–liquid phase equilibria for such mixtures, a number of more theoretically based mixing rules for use with the S–R–K and P–R equations of state have been developed. In a different approach, Holderbaum and Gmehling [58] formulated a group-contribution equation of state referred to as the predictive Soave–Redlich–Kwong (PSRK) model, which combines a modified S–R–K equation of state with the UNIFAC model. To improve the ability of the S–R–K equation to predict vapor pressure of polar compounds, they provide an improved temperature dependence for the pure-component parameter, a, in Table 2.5. To handle mixtures of nonpolar, polar, and supercritical components, they use a mixing rule for a, which includes the UNIFAC model for handling nonideal effects more accurately. Additional and revised pure-component and group interaction parameters for use in the PSRK model are provided by Fischer and Gmehling [59]. In particular, [58] and [59] provide parameters for nine light gases (Ar, CO, CO_2, CH_4, H_2, H_2S, N_2, NH_3, and O_2) in addition to UNIFAC parameters for 50 groups.

Electrolyte Solution Models

Solutions of weak and/or strong electrolytes are common in chemical processes. For example, sour water, found in many petroleum plants, may consist of solvent (water) and five dissolved gases: CO, CO_2, CH_4, H_2S, and NH_3. The apparent composition of the solution is based on these six molecules. However, because of dissociation, which in this case is weak, the true composition of the aqueous solution includes ionic as well as molecular species. For sour water, the ionic species present at chemical equilibrium include H^+, OH^-, HCO_3^-, $CO_3^=$, HS^-, $S^=$, NH_4^+, and NH_2COO^-, with the total numbers of positive and negative ions subject to electroneutrality. For example, while the apparent concentration of NH_4 in the solution might be 2.46 moles per kg of water, when dissociation is taken into account, the molality is only 0.97, with NH_4^+ having a molality of 1.49. All eight ionic species are nonvolatile, while all six molecular species are volatile to some extent. Accurate calculations of vapor–liquid equilibrium for multicomponent electrolyte solutions must consider both chemical and physical equilibrium, both of which involve liquid-phase activity coefficients.

A number of models have been developed for predicting activity coefficients in multicomponent systems of electrolytes. Of particular note are the models of Pitzer [60] and Chen and associates [61, 62, and 63], both of which are included in simulation programs. Both models can handle dilute to concentrated solutions, but only the model of Chen and associates, which is a substantial modification of the NRTL model (see Section 2.6), can handle mixed-solvent systems, such as those containing water and alcohols.

Polymer Solution Models

Polymer processing often involves solutions of solvent, monomer, and an amorphous (noncrystalline) polymer, requiring vapor–liquid and, sometimes, liquid–liquid phase-equilibria calculations, for which estimation of activity coefficients of all components in the mixture is needed. In general, the polymer is nonvolatile, but the solvent and monomer are volatile. When the solution is dilute in the polymer, activity-coefficient methods of Section 2.6, such as the NRTL method, can be used. Of more interest are solutions with appreciable concentrations of polymer, for which the methods of Sections 2.5 and 2.6 are inadequate. Consequently, special-purpose empirical and theoretical models have been developed. One method, which is available in simulation programs, is the modified NRTL model of Chen [64], which combines a modification of the Flory-Huggins equation (12-65) for widely differing molecular size with the NRTL concept of local composition. Chen represents the polymer with segments. Thus, solvent–solvent, solvent–segment, and segment–segment binary interaction parameters are required, which are often available from the literature and may be assumed independent of temperature, polymer chain length, and polymer concentration, making the model quite flexible.

2.8 SELECTING AN APPROPRIATE MODEL

The three previous sections of this chapter have discussed the more widely used models for estimating fugacities, activity coefficients, and K-values for components in mixtures. These models and others are included in computer-aided, process-simulation programs. To solve a particular separations problem, it is necessary to select an appropriate model. This section presents recommendations for making at least a preliminary selection.

The selection procedure includes a few models not covered in this chapter, but for which a literature reference is given. The procedure begins by characterizing the mixture by chemical types present: Light gases (LG), Hydrocarbons (HC), Polar organic compounds (PC), and Aqueous solutions (A), with or without Electrolytes (E).

If the mixture is (A) with no (PC), then if electrolytes are present, select the modified NRTL equation. Otherwise, select a special model, such as one for sour water (containing NH_3, H_2S, CO_2, etc.) or aqueous amine solutions.

If the mixture contains (HC), with or without (LG), covering a wide boiling range, choose the corresponding-states method of Lee–Kesler–Plöcker [8, 65]. If the boiling range of a mixture of (HC) is not wide boiling, the selection depends on the pressure and temperature. For all temperatures and pressures, the Peng–Robinson equation is suitable. For

all pressures and noncryogenic temperatures, the Soave–Redlich–Kwong equation is suitable. For all temperatures, but not pressures in the critical region, the Benedict–Webb–Rubin–Starling [5, 66, 67] method is suitable.

If the mixture contains (PC), the selection depends on whether (LG) are present. If they are, the PSRK method is recommended. If not, then a suitable liquid-phase activity-coefficient method is selected as follows. If the binary interaction coefficients are not available, select the UNIFAC method, which should be considered as only a first approximation. If the binary interaction coefficients are available and splitting in two liquid phases will not occur, select the Wilson or NRTL equation. Otherwise, if phase splitting is probable, select the NRTL or UNIQUAC equation.

SUMMARY

1. Separation processes are often energy-intensive. Energy requirements are determined by applying the first law of thermodynamics. Estimates of minimum energy needs can be made by applying the second law of thermodynamics with an entropy balance or an availability balance.

2. Phase equilibrium is expressed in terms of vapor–liquid and liquid–liquid *K*-values, which are formulated in terms of fugacity and activity coefficients.

3. For separation systems involving an ideal-gas mixture and an ideal-liquid solution, all necessary thermodynamic properties can be estimated from the ideal-gas law, a vapor heat-capacity equation, a vapor-pressure equation, and an equation for the liquid density as a function of temperature.

4. Graphical correlations of pure-component thermodynamic properties are widely available and useful for making rapid, manual calculations at near-ambient pressure for an ideal solution.

5. For nonideal vapor and liquid mixtures containing nonpolar components, certain *P*–*v*–*T* equation-of-state models such as S–R–K, P–R, and L–K–P can be used to estimate density, enthalpy, entropy, fugacity coefficients, and *K*-values.

6. For nonideal liquid solutions containing nonpolar and/or polar components, certain free-energy models such as Margules, van Laar, Wilson, NRTL, UNIQUAC, and UNIFAC can be used to estimate activity coefficients, volume and enthalpy of mixing, excess entropy of mixing, and *K*-values.

7. Special models are available for polymer solutions, electrolyte solutions, and mixtures of polar and supercritical components.

REFERENCES

1. Mix, T.W., J.S. Dweck, M. Weinberg, and R.C. Armstrong, *AIChE Symp. Ser., No. 192,* Vol. 76, 15–23 (1980).
2. Felder, R.M., and R.W. Rousseau, *Elementary Principles of Chemical Processes,* 3rd ed., John Wiley & Sons, New York (2000).
3. de Nevers, N., and J.D. Seader, *Latin Am. J. Heat and Mass Transfer,* **8,** 77–105 (1984).
4. Prausnitz, J.M., R.N. Lichtenthaler, and E.G. de Azevedo, *Molecular Thermodynamics of Fluid-Phase Equilibria,* 3rd ed., Prentice-Hall, Upper Saddle River, NJ (1999).
5. Starling, K.E., *Fluid Thermodynamic Properties for Light Petroleum Systems,* Gulf Publishing, Houston, TX (1973).
6. Soave, G., *Chem. Eng. Sci.,* **27,** 1197–1203 (1972).
7. Peng, D.Y., and D.B. Robinson, *Ind. Eng. Chem. Fundam.,* **15,** 59–64 (1976).
8. Plöcker, U., H. Knapp, and J.M. Prausnitz, *Ind. Eng. Chem. Process Des. Dev.,* **17,** 324–332 (1978).
9. Chao, K.C., and J.D. Seader, *AIChE J.,* **7,** 598–605 (1961).
10. Grayson, H.G., and C.W. Streed, Paper 20-P07, Sixth World Petroleum Conference, Frankfurt, June 1963.
11. Poling, B.E., J.M. Prausnitz, and J.P. O'Connell, *The Properties of Gases and Liquids,* 5th ed., McGraw-Hill, New York (2001).
12. Rackett, H.G., *J. Chem. Eng. Data,* **15,** 514–517 (1970).
13. Yaws, C.L., H.-C. Yang, J.R. Hopper, and W.A. Cawley, *Hydrocarbon Processing,* **71** (1), 103–106 (1991).
14. Frank, J.C., G.R. Geyer, and H. Kehde, *Chem. Eng. Prog.,* **65** (2), 79–86 (1969).
15. Hadden, S.T., and H.G. Grayson, *Hydrocarbon Process., Petrol. Refiner,* **40** (9), 207–218 (1961).
16. Robbins, L.A., Section 15, "Liquid-Liquid Extraction Operations and Equipment," in R.H. Perry, D. Green, and J.O. Maloney, Eds., *Perry's Chemical Engineers' Handbook,* 7th ed., McGraw-Hill, New York (1997).
17. Pitzer, K.S., D.Z. Lippman, R.F. Curl, Jr., C.M. Huggins, and D.E. Petersen, *J. Am. Chem. Soc.,* **77,** 3433–3440 (1955).
18. Redlich, O., and J.N.S. Kwong, *Chem. Rev.,* **44,** 233–244 (1949).
19. Shah, K.K., and G. Thodos, *Ind. Eng. Chem.,* **57** (3), 30–37 (1965).
20. Glanville, J.W., B.H. Sage, and W.N. Lacey, *Ind. Eng. Chem.,* **42,** 508–513 (1950).
21. Wilson, G.M., *Adv. Cryogenic Eng.,* **11,** 392–400 (1966).
22. Knapp, H., R. Doring, L. Oellrich, U. Plöcker, and J.M. Prausnitz, *Vapor-Liquid Equilibria for Mixtures of Low Boiling Substances,* Chem. Data. Ser., Vol. VI, DECHEMA (1982).
23. Thiesen, M., *Ann. Phys.,* **24,** 467–492 (1885).
24. Onnes, K., *Konink. Akad. Wetens,* p. 633 (1912).
25. Walas, S.M., *Phase Equilibria in Chemical Engineering,* Butterworth, Boston (1985).
26. Lee, B.I., and M.G. Kessler, *AIChE J.,* **21,** 510–527 (1975).
27. Edmister, W.C., *Hydrocarbon Processing,* **47** (9), 239–244 (1968).
28. Yarborough, L., *J. Chem. Eng. Data,* **17,** 129–133 (1972).
29. Prausnitz, J.M., W.C. Edmister, and K.C. Chao, *AIChE J.,* **6,** 214–219 (1960).
30. Hildebrand, J.H., J.M. Prausnitz, and R.L. Scott, *Regular and Related Solutions,* Van Nostrand Reinhold, New York (1970).
31. Yerazunis, S., J.D. Plowright, and F.M. Smola, *AIChE J.,* **10,** 660–665 (1964).
32. Hermsen, R.W., and J.M. Prausnitz, *Chem. Eng. Sci.,* **18,** 485–494 (1963).

33. Ewell, R.H., J.M. Harrison, and L. Berg, *Ind. Eng. Chem.,* **36,** 871–875 (1944).

34. Van Ness, H.C., C.A. Soczek, and N.K. Kochar, *J. Chem. Eng. Data,* **12,** 346–351 (1967).

35. Sinor, J.E., and J.H. Weber, *J. Chem. Eng. Data,* **5,** 243–247 (1960).

36. Orye, R.V., and J.M. Prausnitz, *Ind. Eng. Chem.,* **57** (5), 18–26 (1965).

37. Wilson, G.M., *J. Am. Chem. Soc.,* **86,** 127–130 (1964).

38. Cukor, P.M., and J.M. Prausnitz, *Inst. Chem. Eng. Symp. Ser. No. 32,* **3,** 88 (1969).

39. Gmehling, J., and U. Onken, *Vapor-Liquid Equilibrium Data Collection,* DECHEMA Chem. Data Ser., 1–8, (1977–1984).

40. Hiranuma, M., *J. Chem. Eng. Japan,* **8,** 162–163 (1957).

41. Renon, H., and J.M. Prausnitz, *AIChE J.,* **14,** 135–144 (1968).

42. Renon, H., and J.M. Prausnitz, *Ind. Eng. Chem. Process Des. Dev.,* **8,** 413–419 (1969).

43. Abrams, D.S., and J.M. Prausnitz, *AIChE J.,* **21,** 116–128 (1975).

44. Abrams, D.S., Ph.D. thesis in chemical engineering, University of California, Berkeley, 1974.

45. Prausnitz, J.M., T.F. Anderson, E.A. Grens, C.A. Eckert, R. Hsieh, and J.P. O'Connell, *Computer Calculations for Multicomponent Vapor-Liquid and Liquid-Liquid Equilibria,* Prentice-Hall, Englewood Cliffs, NJ (1980).

46. Fredenslund, A., J. Gmehling, M.L. Michelsen, P. Rasmussen, and J.M. Prausnitz, *Ind. Eng. Chem. Process Des. Dev.,* **16,** 450–462 (1977).

47. Wilson, G.M., and C.H. Deal, *Ind. Eng. Chem. Fundam.,* **1,** 20–23 (1962).

48. Derr, E.L., and C.H. Deal, *Inst. Chem. Eng. Symp. Ser. No. 32,* **3,** 40–51 (1969).

49. Fredenslund, A., R.L. Jones, and J.M. Prausnitz, *AIChE J.,* **21,** 1086–1099 (1975).

50. Fredenslund, A., J. Gmehling, and P. Rasmussen, *Vapor-Liquid Equilibria Using UNIFAC, A Group Contribution Method,* Elsevier, Amsterdam (1977).

51. Gmehling, J., P. Rasmussen, and A. Fredenslund, *Ind. Eng. Chem. Process Des. Dev.,* **21,** 118–127 (1982).

52. Larsen, B.L., P. Rasmussen, and A. Fredenslund, *Ind. Eng. Chem. Res.,* **26,** 2274–2286 (1987).

53. Gmehling, J., J. Li, and M. Schiller, *Ind. Eng. Chem. Res.,* **32,** 178–193 (1993).

54. Wittig, R., J. Lohmann, and J. Gmehling, *Ind. Eng. Chem. Res.,* **42,** 183–188 (2003).

55. Takeuchi, S., T. Nitta, and T. Katayama, *J. Chem. Eng. Japan,* **8,** 248–250 (1975).

56. Strubl, K., V. Svoboda, R. Holub, and J. Pick, *Collect. Czech. Chem. Commun.,* **35,** 3004–3019 (1970).

57. Kiser, R.W., G.D. Johnson, and M.D. Shetlar, *J. Chem. Eng. Data,* **6,** 338–341 (1961).

58. Holderbaum, T., and J. Gmehling, *Fluid Phase Equilibria,* **70,** 251–265 (1991).

59. Fischer, K., and J. Gmehling, *Fluid Phase Equilibria,* **121,** 185–206 (1996).

60. Pitzer, K.S., *J. Phys. Chem.,* **77,** No. 2, 268–277 (1973).

61. Chen, C.-C., H.I. Britt, J.F. Boston, and L.B. Evans, *AIChE Journal,* **28,** 588–596 (1982).

62. Chen, C.-C., and L.B. Evans, *AIChE Journal,* **32,** 444–459 (1986).

63. Mock, B., L.B. Evans, and C.-C. Chen, *AIChE Journal,* **28,** 1655–1664 (1986).

64. Chen, C.-C., *Fluid Phase Equilibria,* **83,** 301–312 (1993).

65. Lee, B.I., and M.G. Kesler, *AIChE Journal,* **21,** 510–527 (1975).

66. Benedict, M., G.B. Webb, and L.C. Rubin, *Chem. Eng. Progress,* **47** (8), 419 (1951).

67. Benedict, M., G.B. Webb, and L.C. Rubin, *Chem. Eng. Progress,* **47** (9), 449 (1951).

EXERCISES

Section 2.1

2.1 A hydrocarbon stream in a petroleum refinery is to be separated at 1,500 kPa into two products under the conditions shown below. Using the data given, compute the minimum work of separation, $W_{\min}$, in kJ/h for $T_0 = 298.15$ K.

	kmol/h	
Component	Feed	Product 1
Ethane	30	30
Propane	200	192
n-Butane	370	4
n-Pentane	350	0
n-Hexane	50	0

	Feed	Product 1	Product 2
Phase condition	Liquid	Vapor	Liquid
Temperature, K	364	313	394
Enthalpy, kJ/kmol	19,480	25,040	25,640
Entropy, kJ/kmol-K	36.64	33.13	54.84

2.2 In petroleum refineries, a mixture of paraffins and cycloparaffins is commonly reformed in a fixed-bed catalytic reactor to produce blending stocks for gasoline and aromatic precursors for making petrochemicals. A typical multicomponent product from catalytic reforming is a mixture of ethylbenzene with the three xylene isomers. If this mixture is separated, these four chemicals can then be subsequently processed to make styrene, phthalic anhydride, isophthalic acid, and terephthalic acid. Compute, using the following data, the minimum work of separation in Btu/h for $T_0 = 560°$R if the mixture below is separated at 20 psia into three products.

		Split Fraction (SF)		
Component	Feed, lbmol/h	Product 1	Product 2	Product 3
Ethylbenzene	150	0.96	0.04	0.000
p-Xylene	190	0.005	0.99	0.005
m-Xylene	430	0.004	0.99	0.006
o-Xylene	230	0.00	0.015	0.985

	Feed	Product 1	Product 2	Product 3
Phase condition	Liquid	Liquid	Liquid	Liquid
Temperature, °F	305	299	304	314
Enthalpy, Btu/lbmol	29,290	29,750	29,550	28,320
Entropy, Btu/lbmol-°R	15.32	12.47	13.60	14.68

2.3 Distillation column C3 in Figure 1.9 separates stream 5 into streams 6 and 7, according to the material balance in Table 1.5. A suitable column for the separation, if carried out at 700 kPa, contains 70 plates with a condenser duty of 27,300,000 kJ/h. Using the following data and an infinite surroundings temperature, T_0, of 298.15 K, compute:

(a) The duty of the reboiler in kJ/h

(b) The irreversible production of entropy in kJ/h-K, assuming the use of cooling water at a nominal temperature of 25°C for the condenser and saturated steam at 100°C for the reboiler

(c) The lost work in kJ/h

(d) The minimum work of separation in kJ/h

(e) The second-law efficiency

Assume the shaft work of the reflux pump is negligible.

	Feed (Stream 5)	Distillate (Stream 6)	Bottoms (Stream 7)
Phase condition	Liquid	Liquid	Liquid
Temperature, K	348	323	343
Pressure, kPa	1,950	700	730
Enthalpy, kJ/kmol	17,000	13,420	15,840
Entropy, kJ/kmol-K	25.05	5.87	21.22

2.4 A spiral-wound, nonporous cellulose acetate membrane separator is to be used to separate a gas containing H_2, CH_4, and C_2H_6. The permeate will be 95 mol% pure H_2 and will contain no ethane. The relative split ratio (separation power), SP, for H_2 relative to methane will be 47. Using the following data and an infinite surroundings temperature of 80°F, compute:

(a) The irreversible production of entropy in Btu/h-R

(b) The lost work in Btu/h

(c) The minimum work of separation in Btu/h. Why is it negative?

What other method(s) might be used to make the separation?

	Feed flow rates, lbmol/h
H_2	3,000
CH_4	884
C_2H_6	120

Stream properties:

	Feed	Permeate	Retentate
Phase condition	Vapor	Vapor	Vapor
Temperature, °F	80	80	80
Pressure, psia	365	50	365
Enthalpy, Btu/lbmol	8,550	8,380	8,890
Entropy, Btu/lbmol-R	1.520	4.222	2.742

Section 2.2

2.5 Which of the following *K*-value expressions, if any, is (are) rigorous? For those expressions that are not rigorous, cite the assumptions involved.

(a) $K_i = \bar{\phi}_{iL}/\bar{\phi}_{iV}$

(b) $K_i = \phi_{iL}/\phi_{iL}$

(c) $K_i = \phi_{iL}$

(d) $K_i = \gamma_{iL}\phi_{iL}/\bar{\phi}_{iV}$

(e) $K_i = P_i^s/P$

(f) $K_i = \gamma_{iL}\phi_{iL}/\gamma_{iV}\phi_{iV}$

(g) $K_i = \gamma_{iL}P_i^s/P$

2.6 Experimental measurements of Vaughan and Collins [*Ind. Eng. Chem.,* **34,** 885 (1942)] for the propane–isopentane system at 167°F and 147 psia show for propane a liquid-phase mole fraction of 0.2900 in equilibrium with a vapor-phase mole fraction of 0.6650. Calculate:

(a) The *K*-values for C_3 and iC_5 from the experimental data.

(b) Estimates of the *K*-values of C_3 and iC_5 from Raoult's law assuming vapor pressures at 167°F of 409.6 and 58.6 psia, respectively.

Compare the results of (a) and (b). Assuming the experimental values are correct, how could better estimates of the *K*-values be achieved? To respond to this question, compare the rigorous expression $K_i = \gamma_{iL}\phi_{iL}/\bar{\phi}_{iV}$ to the Raoult's law expression $K_i = P_i^s/P$.

2.7 Mutual solubility data for the isooctane (1)/furfural (2) system at 25°C are [*Chem. Eng. Sci.*, **6,** 116 (1957)]

	Liquid Phase I	Liquid Phase II
x_1	0.0431	0.9461

Compute:

(a) The distribution coefficients for isooctane and furfural

(b) The relative selectivity for isooctane relative to furfural

(c) The activity coefficient of isooctane in liquid phase 1 and the activity coefficient of furfural in liquid phase 2 assuming $\gamma_2^{(1)} = 1.0$ and $\gamma_1^{(2)} = 1.0$.

2.8 In petroleum refineries, streams rich in alkylbenzenes and alkylnaphthalenes result from catalytic cracking operations. Such streams can be hydrodealkylated to more valuable products such as benzene and naphthalene. At 25°C, solid naphthalene (normal melting point = 80.3°C) has the following solubilities in various liquid solvents [*Naphthalene,* API Publication 707, Washington, DC (Oct. 1978)], including benzene:

Solvent	Mole Fraction Naphthalene
Benzene	0.2946
Cyclohexane	0.1487
Carbon tetrachloride	0.2591
n-Hexane	0.1168
Water	0.18×10^{-5}

For each solvent, compute the activity coefficient of naphthalene in the liquid solvent phase using the following equations for the vapor pressure in torr of solid and liquid naphthalene:

$$\ln P^s_{\text{solid}} = 26.708 - 8{,}712/T$$

$$\ln P^s_{\text{liquid}} = 16.1426 - 3992.01/(T - 71.29)$$

where T is in K.

Section 2.3

2.9 A binary ideal-gas mixture of A and B undergoes an isothermal, isobaric separation at T_0, the infinite surroundings temperature. Starting with Eq. (4), Table 2.1, derive an equation for the minimum work of separation, W_{min}, in terms of mole fractions of the feed and the two products. Use your equation to prepare a plot of the dimensionless group, W_{min}/RT_0n_F, as a function of mole fraction of A in the feed for:

(a) A perfect separation

(b) A separation with $SF_A = 0.98$, $SF_B = 0.02$

(c) A separation with $SR_A = 9.0$ and $SR_B = \frac{1}{9}$

(d) A separation with $SF = 0.95$ for A and $SP_{A,B} = 361$

How sensitive is W_{min} to product purities? Does W_{min} depend on the particular separation operation used?

Prove, by calculus, that the largest value of W_{min} occurs for a feed with equimolar quantities of A and B.

2.10 The separation of isopentane from *n*-pentane by distillation is difficult (approximately 100 trays are required), but is commonly practiced in industry. Using the extended Antoine vapor pressure equation, (2-39), with the constants below and in conjunction with Raoult's law, calculate relative volatilities for the isopentane/*n*-pentane system and compare the values on a plot with the following smoothed experimental values [*J. Chem. Eng. Data,* **8,** 504 (1963)]:

Temperature, °F	α_{iC_5,nC_5}
125	1.26
150	1.23
175	1.21
200	1.18
225	1.16
250	1.14

What do you conclude about the applicability of Raoult's law in this temperature range for this binary system?

Vapor pressure constants for (2-39) with vapor pressure in kPa and T in K are

	iC_5	nC_5
k_1	13.6106	13.9778
k_2	−2,345.09	−2,554.60
k_3	−40.2128	−36.2529
k_4, k_5, k_6	0	0

2.11 Operating conditions at the top of a vacuum distillation column for the separation of ethylbenzene from styrene are given below, where the overhead vapor is condensed in an air-cooled condenser to give subcooled reflux and distillate. Using the property constants in Example 2.3, estimate the heat transfer rate (duty) for the condenser in kJ/h, assuming an ideal gas and ideal gas and liquid solutions.

	Overhead Vapor	Reflux	Distillate
Phase condition	Vapor	Liquid	Liquid
Temperature, K	331	325	325
Pressure, kPa	6.69	6.40	6.40
Component flow rates, kg/h:			
Ethylbenzene	77,500	66,960	10,540
Styrene	2,500	2,160	340

2.12 Toluene can be hydrodealkylated to benzene, but the conversion per pass through the reactor is only about 70%. Consequently, the toluene must be recovered and recycled. Typical conditions for the feed to a commercial distillation unit are 100°F, 20 psia, 415 lbmol/h of benzene, and 131 lbmol/h of toluene. Based on the property constants below, and assuming that the ideal gas, ideal liquid solution model of Table 2.4 applies at this low pressure, prove that the mixture is a liquid and estimate v_L and ρ_L in American engineering units.

Property constants for (2-38) and (2-39), where in all cases, T is in K, are

	Benzene	Toluene
M, kg/kmol	78.114	92.141
P^s, torr:		
k_1	15.9008	16.0137
k_2	−2,788.51	−3,096.52
k_3	−52.36	−53.67
k_4, k_5, k_6	0	0
ρ_L, kg/m^3:		
A	304.1	290.6
B	0.269	0.265
T_c	562.0	593.1

Section 2.4

2.13 Measured conditions for the bottoms from a depropanizer distillation unit in a small refinery are given below. Using the data in Figure 2.3 and assuming an ideal liquid solution (volume of mixing = 0), compute the liquid density in lb/ft^3, lb/gal, lb/bbl (42 gal), and kg/m^3.

Phase Condition	Liquid
Temperature, °F	229
Pressure, psia	282
Flow rates, lbmol/h:	
C_3	2.2
iC_4	171.1
nC_4	226.6
iC_5	28.1
nC_5	17.5

2.14 Isopropanol, containing 13 wt% water, can be dehydrated to obtain almost pure isopropanol at a 90% recovery by azeotropic distillation with benzene. When condensed, the overhead vapor from the column splits into two immiscible liquid phases. Use the relations in Table 2.4 with data in Perry's Handbook and the operating conditions below to compute the rate of heat transfer in Btu/h and kJ/h for the condenser.

	Overhead	Water-Rich Phase	Organic-Rich Phase
Phase	Vapor	Liquid	Liquid
Temperature, °C	76	40	40
Pressure, bar	1.4	1.4	1.4
Flow rate, kg/h:			
Isopropanol	6,800	5,870	930
Water	2,350	1,790	560
Benzene	24,600	30	24,570

2.15 A hydrocarbon vapor–liquid mixture at 250°F and 500 psia contains N_2, H_2S, CO_2, and all the normal paraffins from methane to heptane. Use Figure 2.8 to estimate the *K*-value of each

component in the mixture. Which components will have a tendency to be present to a greater extent in the equilibrium vapor?

2.16 Acetone, a valuable solvent, can be recovered from air by absorption in water or by adsorption on activated carbon. If absorption is used, the conditions for the streams entering and leaving are as listed below. If the absorber operates adiabatically, estimate the temperature of the exiting liquid phase using a simulation program.

	Feed Gas	Absorbent	Gas Out	Liquid Out
Flow rate, lbmol/h:				
Air	687	0	687	0
Acetone	15	0	0.1	14.9
Water	0	1,733	22	1,711
Temperature, °F	78	90	80	—
Pressure, psia	15	15	14	15
Phase	Vapor	Liquid	Vapor	Liquid

Some concern has been expressed about the possible explosion hazard associated with the feed gas. The lower and upper flammability limits for acetone in air are 2.5 and 13 mol%, respectively. Is the mixture within the explosive range? If so, what can be done to remedy the situation?

Section 2.5

2.17 Subquality natural gas contains an intolerable amount of nitrogen impurity. Separation processes that can be used to remove nitrogen include cryogenic distillation, membrane separation, and pressure-swing adsorption. For the latter process, a set of typical feed and product conditions is given below. Assume a 90% removal of N_2 and a 97% methane natural-gas product. Using the R–K equation of state with the constants listed below, compute the flow rate in thousands of actual cubic feet per hour for each of the three streams.

	N_2	CH_4
Feed flow rate, lbmol/h:	176	704
T_c, K	126.2	190.4
P_c, bar	33.9	46.0

Stream conditions are

	Feed (Subquality Natural Gas)	Product (Natural Gas)	Waste Gas
Temperature, °F	70	100	70
Pressure, psia	800	790	280

2.18 Use the R–K equation of state to estimate the partial fugacity coefficients of propane and benzene in the vapor mixture of Example 2.5.

2.19 Use a computer-aided, steady-state simulation program to estimate the *K*-values, using the P–R and S–R–K equations of state, of an equimolar mixture of the two butane isomers and the four butene isomers at 220°F and 276.5 psia. Compare these values with the following experimental results [*J. Chem. Eng. Data,* **7,** 331 (1962)]:

Component	*K*-value
Isobutane	1.067
Isobutene	1.024
n-Butane	0.922
1-Butene	1.024
trans-2-Butene	0.952
cis-2-Butene	0.876

2.20 The disproportionation of toluene to benzene and xylenes is carried out in a catalytic reactor at 500 psia and 950°F. The reactor effluent is cooled in a series of heat exchangers for heat recovery until a temperature of 235°F is reached at a pressure of 490 psia. The effluent is then further cooled and partially condensed by the transfer of heat to cooling water in a final exchanger. The resulting two-phase equilibrium mixture at 100°F and 485 psia is then separated in a flash drum. For the reactor effluent composition given below, use a computer-aided, steady-state simulation program with the S–R–K and P–R equations of state to compute the component flow rates in lbmol/h in both the resulting vapor and liquid streams, the component *K*-values for the equilibrium mixture, and the rate of heat transfer to the cooling water. Compare the results.

Component	Reactor Effluent, lbmol/h
H_2	1,900
CH_4	215
C_2H_6	17
Benzene	577
Toluene	1,349
p-Xylene	508

Section 2.6

2.21 For an ambient separation process where the feed and products are all nonideal liquid solutions at the infinite surroundings temperature, T_0, (4) of Table 2.1 for the minimum work of separation reduces to

$$\frac{W_{\min}}{RT_0} = \sum_{\text{out}} n \left[\sum_i x_i \ln(\gamma_i x_i) \right] - \sum_{\text{in}} n \left[\sum_i x_i \ln(\gamma_i x_i) \right]$$

For the liquid-phase separation at ambient conditions (298 K, 101.3 kPa) of a 35 mol% mixture of acetone (1) in water (2) into 99 mol% acetone and 98 mol% water products, calculate the minimum work in kJ/kmol of feed. Liquid-phase activity coefficients at ambient conditions are correlated reasonably well by the van Laar equations with $A_{12} = 2.0$ and $A_{21} = 1.7$. What would the minimum rate of work be if acetone and water formed an ideal liquid solution?

2.22 The sharp separation of benzene and cyclohexane by distillation at ambient pressure is impossible because of the formation of an azeotrope at 77.6°C. K.C. Chao [Ph.D. thesis, University of Wisconsin (1956)] obtained the following vapor–liquid equilibrium data for the benzene (B)/cyclohexane (CH) system at 1 atm:

T, °C	x_B	y_B	γ_B	γ_{CH}
79.7	0.088	0.113	1.300	1.003
79.1	0.156	0.190	1.256	1.008
78.5	0.231	0.268	1.219	1.019
78.0	0.308	0.343	1.189	1.032
77.7	0.400	0.422	1.136	1.056
77.6	0.470	0.482	1.108	1.075
77.6	0.545	0.544	1.079	1.102
77.6	0.625	0.612	1.058	1.138
77.8	0.701	0.678	1.039	1.178
78.0	0.757	0.727	1.025	1.221
78.3	0.822	0.791	1.018	1.263
78.9	0.891	0.863	1.005	1.328
79.5	0.953	0.938	1.003	1.369

Vapor pressure is given by (2-39), where constants for benzene are in Exercise 2.12 and constants for cyclohexane are $k_1 = 15.7527$, $k_2 = -2766.63$, and $k_3 = -50.50$.

(a) Use the data to calculate and plot the relative volatility of benzene with respect to cyclohexane versus benzene composition in the liquid phase. What happens to the relative volatility in the vicinity of the azeotrope?

(b) From the azeotropic composition for the benzene/cyclohexane system, calculate the constants in the van Laar equation. With these constants, use the van Laar equation to compute the activity coefficients over the entire range of composition and compare them, in a plot like Figure 2.16, with the above experimental data. How well does the van Laar equation predict the activity coefficients?

2.23 Benzene can be used to break the ethanol/water azeotrope so as to produce nearly pure ethanol. The Wilson constants for the ethanol(1)/benzene(2) system at 45°C are $\Lambda_{12} = 0.124$ and $\Lambda_{21} = 0.523$. Use these constants with the Wilson equation to predict the liquid-phase activity coefficients for this system over the entire range of composition and compare them, in a plot like Figure 2.16, with the following experimental results [*Austral. J. Chem.,* **7,** 264 (1954)]:

x_1	$\ln \gamma_1$	$\ln \gamma_2$
0.0374	2.0937	0.0220
0.0972	1.6153	0.0519
0.3141	0.7090	0.2599
0.5199	0.3136	0.5392
0.7087	0.1079	0.8645
0.9193	0.0002	1.3177
0.9591	−0.0077	1.3999

2.24 For the binary system ethanol(1)/isooctane(2) at 50°C, the infinite-dilution, liquid-phase activity coefficients are $\gamma_1^\infty = 21.17$ and $\gamma_2^\infty = 9.84$.

(a) Calculate the constants A_{12} and A_{21} in the van Laar equations.

(b) Calculate the constants Λ_{12} and Λ_{21} in the Wilson equations.

(c) Using the constants from (a) and (b), calculate γ_1 and γ_2 over the entire composition range and plot the calculated points as log γ versus x_1.

(d) How well do the van Laar and Wilson predictions agree with the azeotropic point where $x_1 = 0.5941$, $\gamma_1 = 1.44$, and $\gamma_2 = 2.18$?

(e) Show that the van Laar equation erroneously predicts separation into two liquid phases over a portion of the composition range by calculating and plotting a y–x diagram like Figure 2.20.